A review of (sub)mm band science and instruments in the ALMA era

Marcella Massardi

INAF- Istituto di Radioastronomia

Italian node of European ALMA Regional Centre

ALMA

EUROPEAN ARC

ALMA Regional Centre || Italian

SISSA – December 2015

Outline

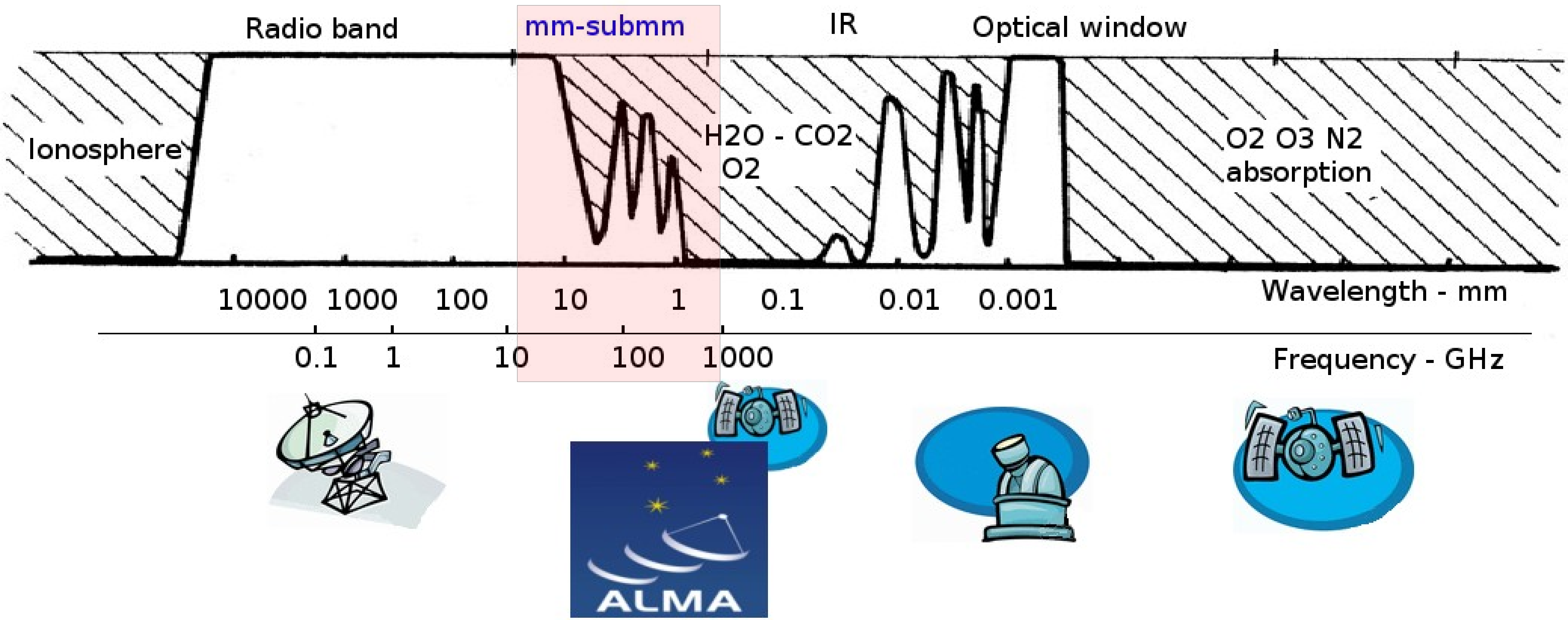

Observing instruments: **Interferometers (ALMA)**

Science topics

Science cases

Observing processes: **Proposals and archives**

Extragalactic science in (sub)mm

The (submm) bands encompass the RJ region of the warm dust thermal emission and the high frequency tail of the synchrotron emission (dominating the radio emission in most galaxies).

The warm dust emitting at far–IR wavelengths is mostly heated by the UV-radiation field of young massive stars in star forming regions.

The far infrared luminosity is considered good tracer of star formation in galaxies.

The spectrum of each galaxy in the submm is rich of rotational molecular transition ladders and atomic fine structure lines, which shapes and relative abundances can be used to trace physical and dynamical properties of the ISM and the mechanisms of SF and AGN activity.

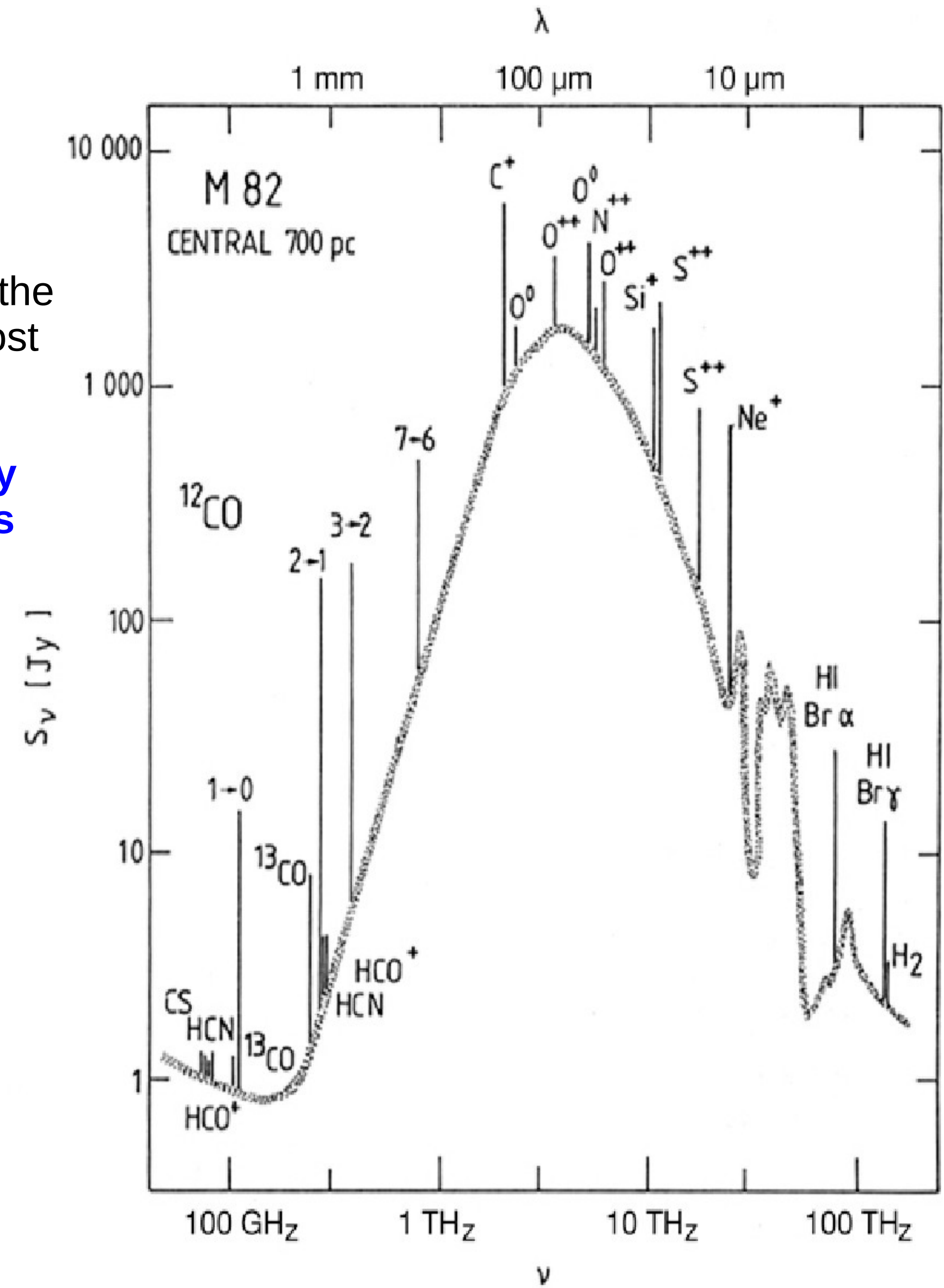

Extragalactic science in (sub)mm

At high redshift the prominent **IR dust thermal bump** (which dominates the SED in starburst galaxies) is shifted into the submm band.

Negative k correction: for 1<z<10 galaxy flux density remain constant for 0.8<λ<2mm. High-z galaxies look brighter than low-z & more high_z than low_z in deep fields.

Obscuration is not an issue as in optical bands

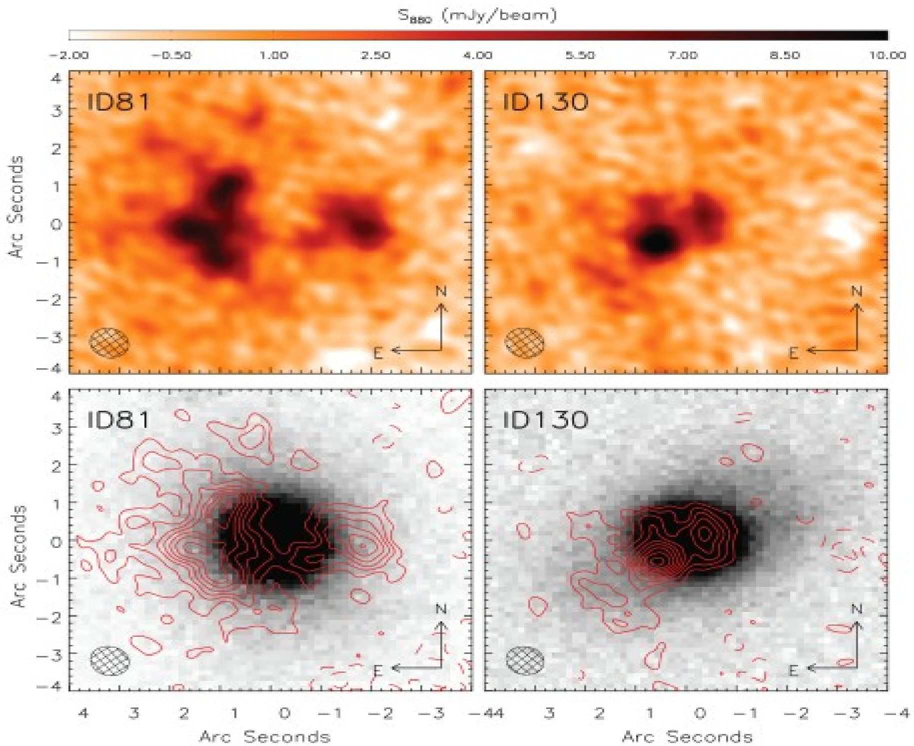

(Negrello et al 2010)

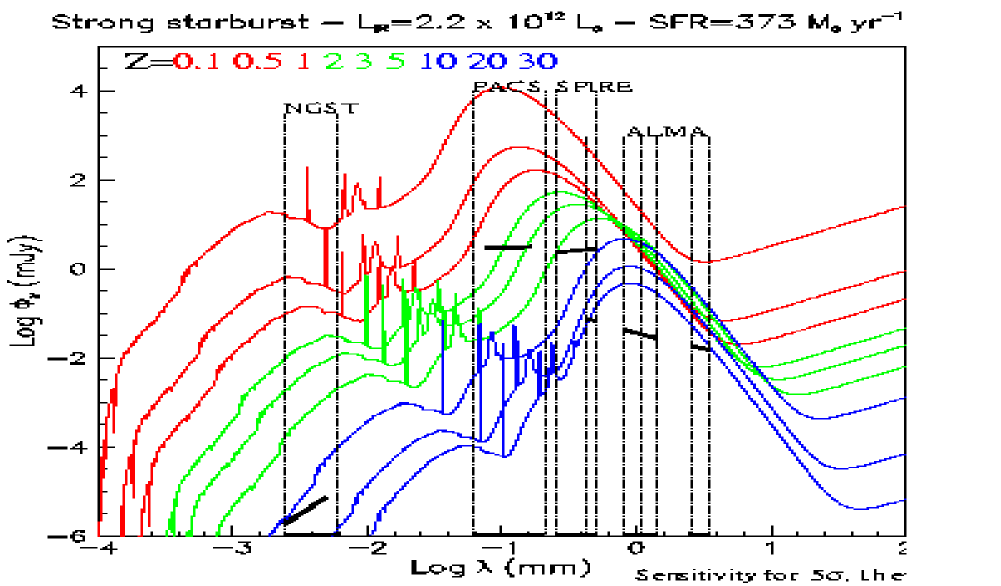

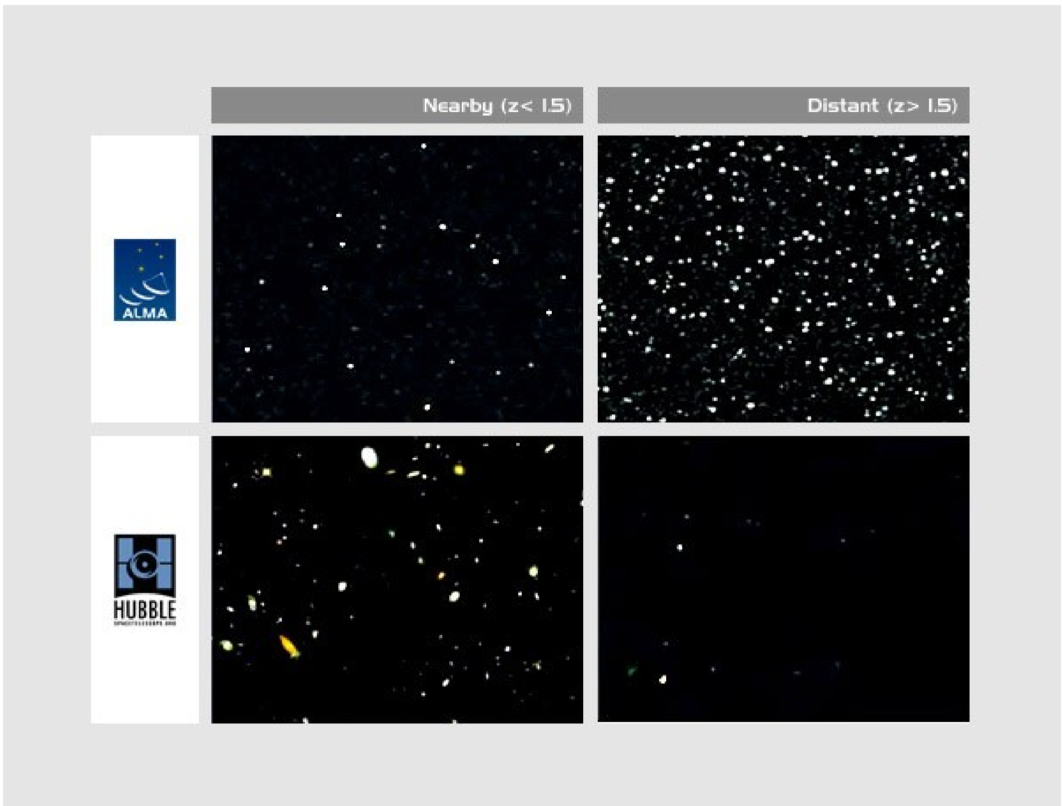

Molecular lines

Molecular rotational transitions are diagnostics of the chemistry, physics and dynamics of the Inter Stellar Medium (ISM) from which stars form.

Some of these lines are so strong
(e.g. the CO transitions)
to be observable even in distant galaxies.

Some of the strongest lines emitted by the ISM of any galaxy, such as the [CII]158 μm and the [OI]63 μm fine structure lines (the two main coolants of the ISM), are redshifted into the (sub)mm bands at z > 2–4

HCN, HCO+ and other high density tracers are powerful tools to distinguish PDR (associated to SF regions) from XDR (associated to AGN).

In most of the ALMA band more than one line is observable for the higher redshifts.

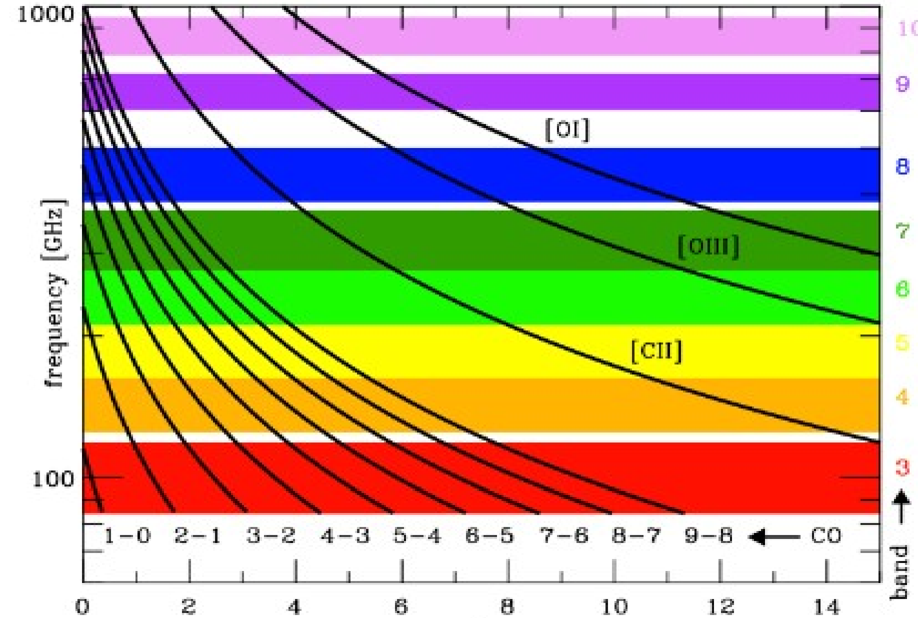

(Maiolino 2008)

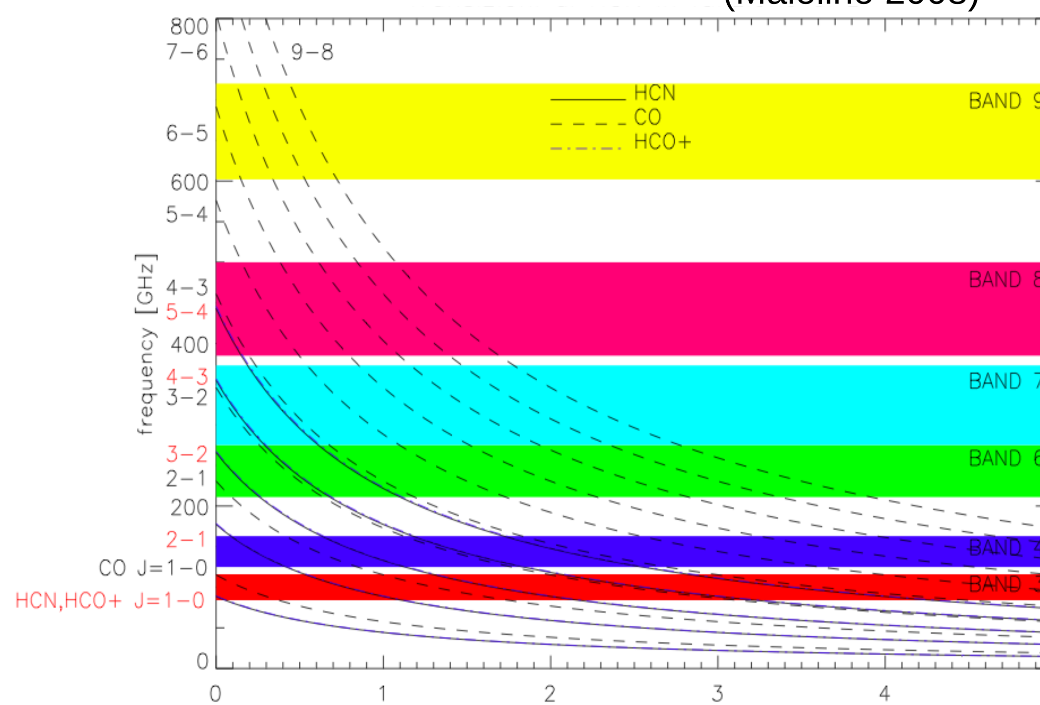

(Courtesy by Bianchi)

CO

- single gas component
- QSO turnover: J > 6-5
- SMG turnover: J ~ 5-4

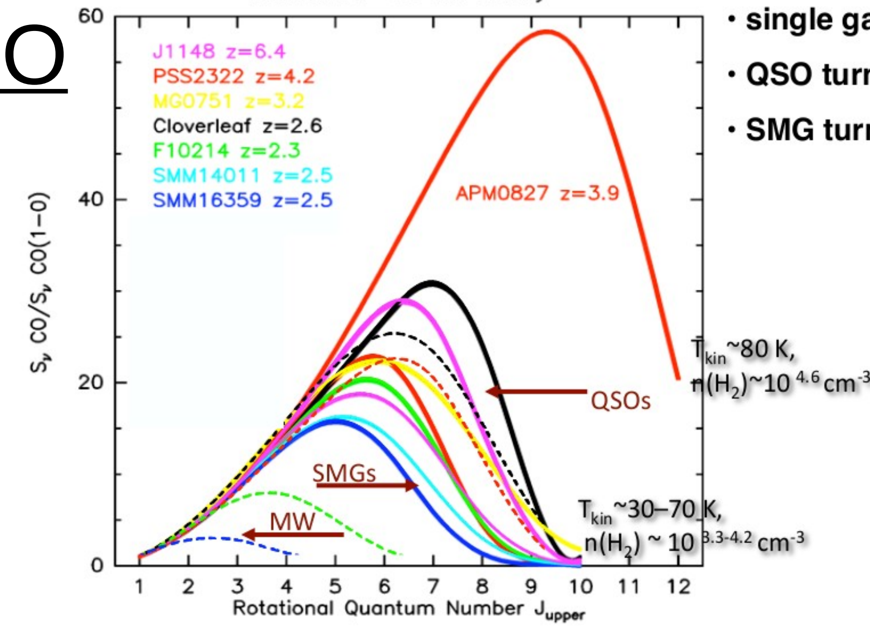

L_CO is proportional to the gas mass (via the relation with H2), L_FIR to the SFR.

$$\log L_{\rm FIR} = 1.7 \log L'_{\rm CO} - 5.0$$

The efficiency of SF grews faster than mass, Hence massive galaxies exhaust their gas faster because of SF.

At high-z the relation is still linear, but with a different slope for SMG and QSO (i.e. different evolution?)

Different CO lines are sensitive to different environment (because of critical density increases with J)

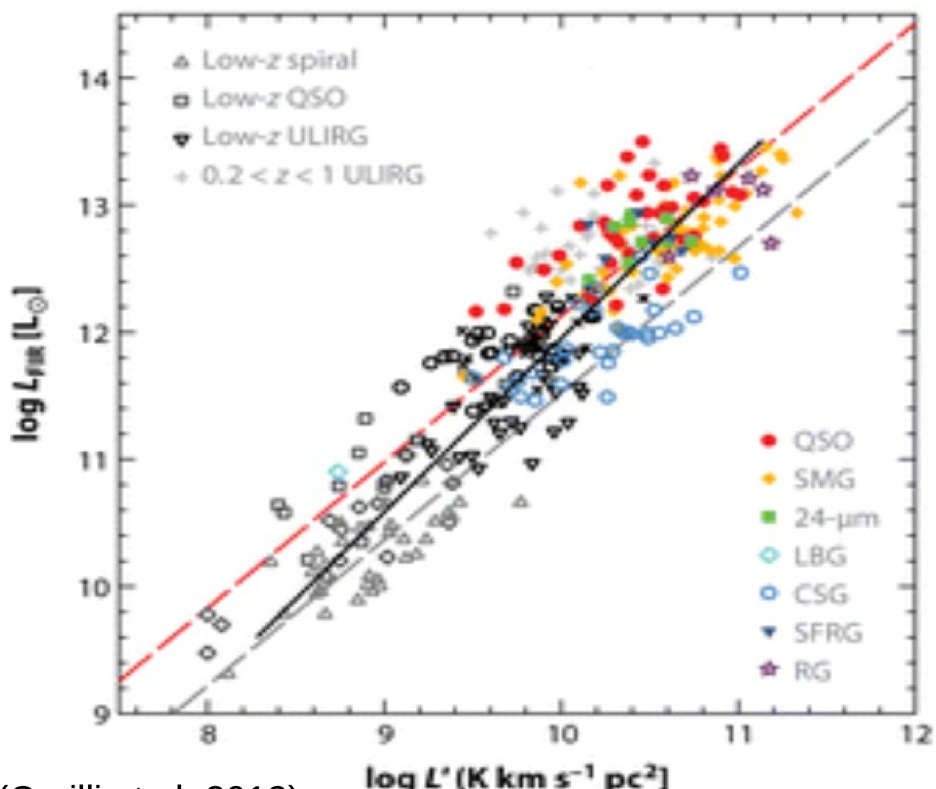

(Carilli et al. 2013)

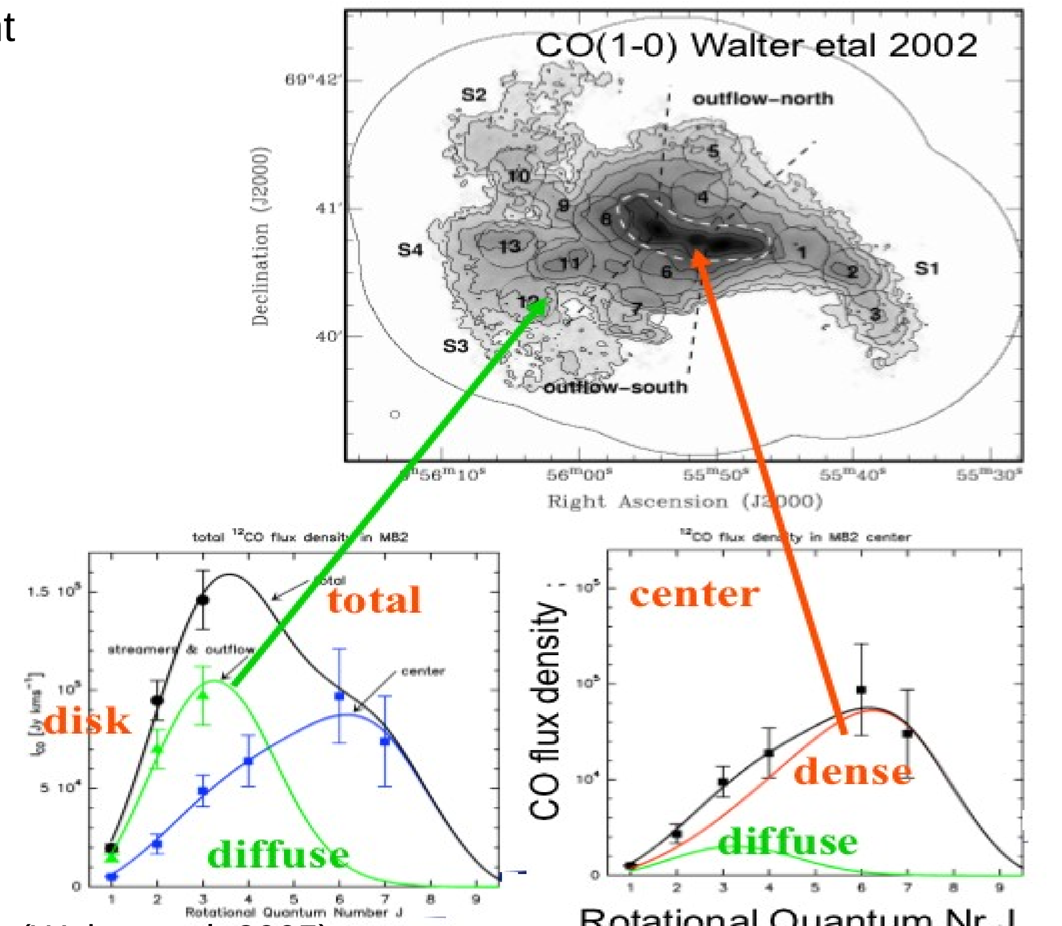

(Weiss et al. 2005)

AGN

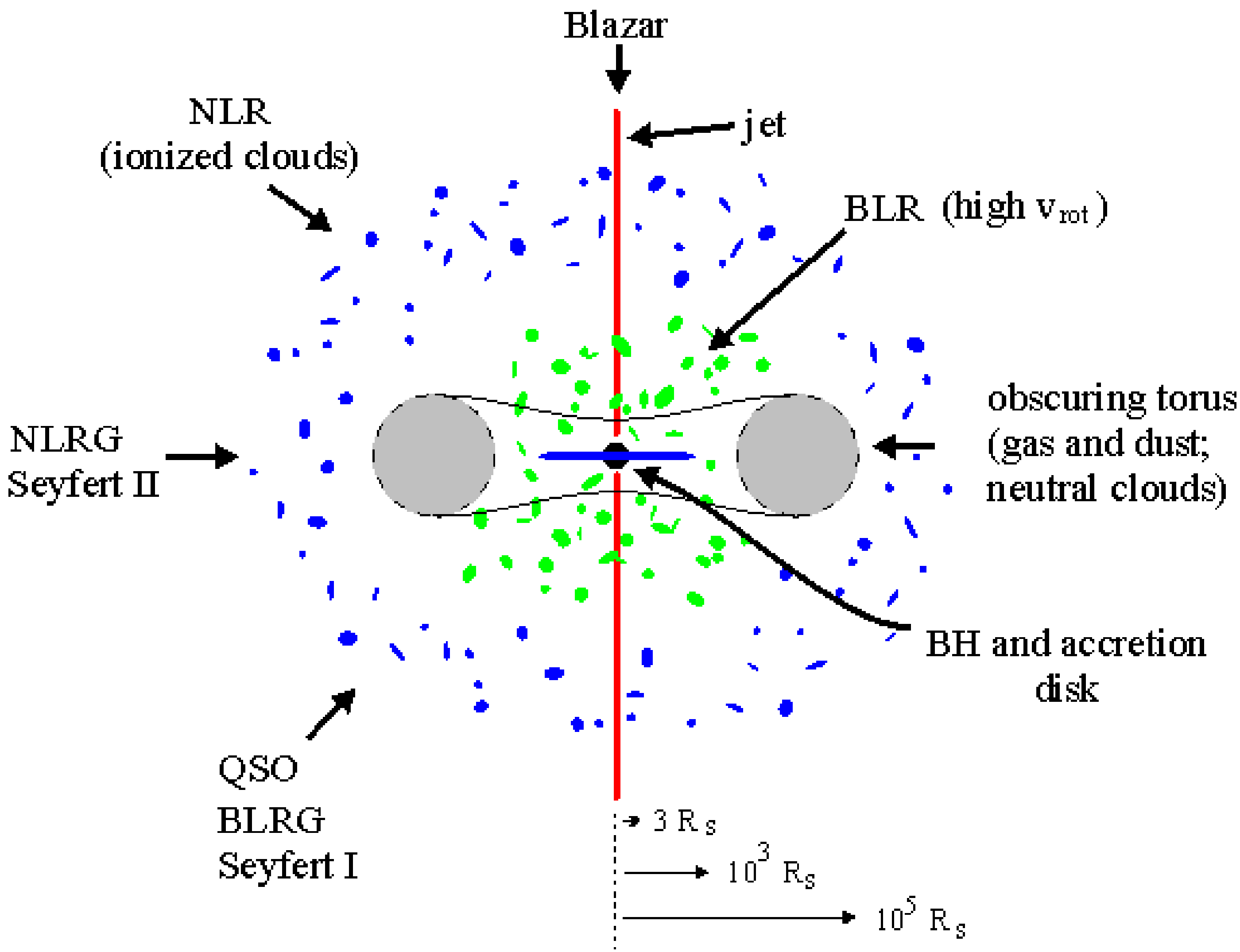

NOTES on SCALES

BLR< 0.1pc
(velocities $10^{3\text{-}4}$km/s)
Torus 1-5 pc
NLR 100 pc
Jet <1Mpc

10marcsec (the ALMA resolution element @300 GHz) correspond to
@z=0.1 10pc
@z=0.5-3 40-60pc

In CenA (z=0.018) → 0.4pc
In NGC1068 (z=0.037) → 0.8pc

AGN Fuelling

Fuelling is the mechanism in which matter accrete on the AGN, removing its angular momentum, feeding the BH and triggering the nuclear activity.

Some theories consider AGN driven by mergers. However, locally there is no strict relation between presence of AGN, companions or barred structures.

Local AGNs do not show obvious systematic signatures of nuclear fuelling from the host galaxy.

Therefore, it is important to trace the dynamics of the molecular gas in the host of these powerful QSOs, and investigate for instance whether in these systems gas funneled by bars or driven by galaxy merging is common.

The CO distribution presents several possible features (see the NUGA survey @ 50-100pc resolution).
Hence AGN do not need fuelling?
For local Seyfert 10^{-3} m_sun/yr (one molecular cloud) can activate the nucleus for 1 Gyr.
For QSOs we need 1M_sun/yr.

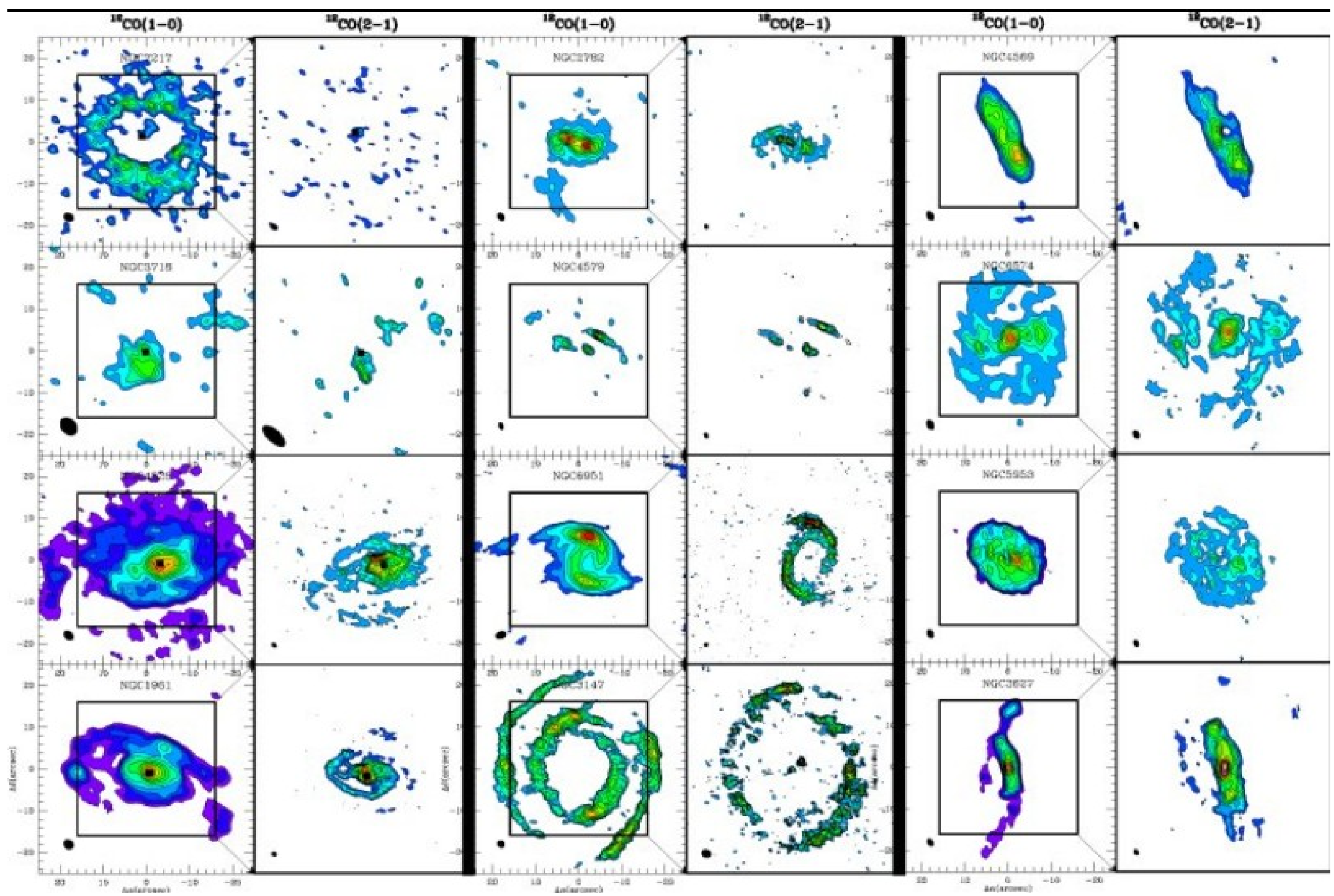

AGN Tori

The circumnuclear molecular medium is both responsible for the obscuration of AGNs and related to their feeding. Models predict:

- a **uniform gas distribution in a toroidal geometry** whose thickness is supported
  by IR radiation pressure (e.g. Krolik, 2007).
  A strong radial temperature gradient is expected for dust and, therefore, the innermost
  warm dust should emit much at higher submm frequencies, than the cold dust in the outer regions.
  Motion is dominated by rotation
- **a clumpy structure originated by the outflow of the accretion disk** (Elitzur et al. 2006).
  Each individual cloud spans a wide range of temperatures and emits at all wavelengths.
  Hence, the nuclear "torus", should show the same morphology at all infrared wavelengths.
  Turbulent components and outflow should trace the dynamics

For closer AGN subpc scale observations can disentangle the models and spectroscopy can trace the tori dynamics. Resolving the gas dynamics allows to directly measure the BH masses

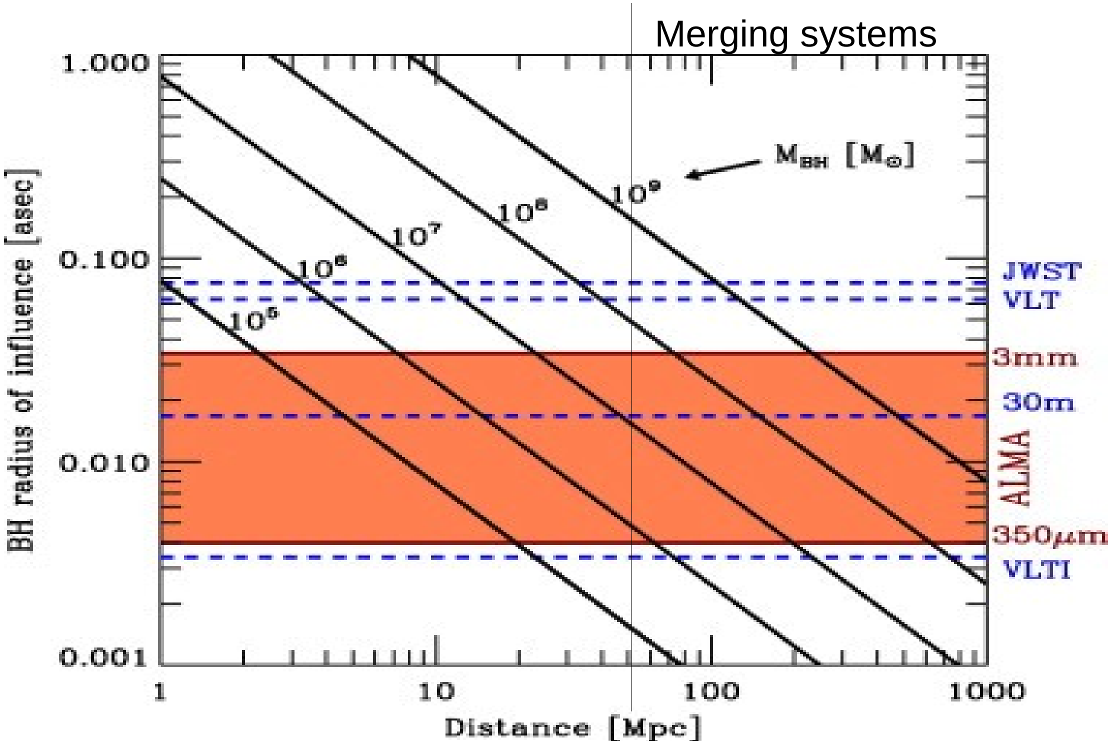

NOTES on SCALES

Torus 1-5 pc

ALMA resolution element (10marcsec @300 Ghz)

In CenA (z=0.018) → 0.4pc
In NGC1068 (z=0.037) → 0.8pc

ALMA observations of NGC1068

NGC1068 is a prototypical Seyfert 2 at D=14 Mpc

- Proposed feeding of the AGN through bars
- Proposed AGN outflow
- Previous PdBI/SMA observations ambiguous interpretation of the kinematics of the inner 50 pc, closer to the AGN

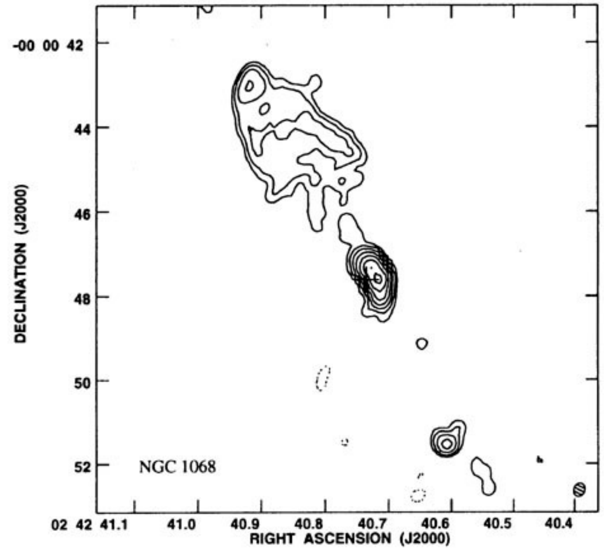

- ➢ Band 7 (350GHz) CO(3-2), HCN, HCO+(4-3), CS(7-6)
- ➢ ~18-27 antennas,
- ➢ ~138min (11 pointing mosaic)
- ➢ Resolution ~ 0.6''x0.5''=35 pc

- ➢ Band 9 (690GHz) CO(6-5)
- ➢ ~21-27 antennas,
- ➢ ~52min (1 pointing)
- ➢ Resolution ~ 0.4''x0.2''=20 pc

(Garcia-Burrillo et al. 2014, Viti et al. 2014)

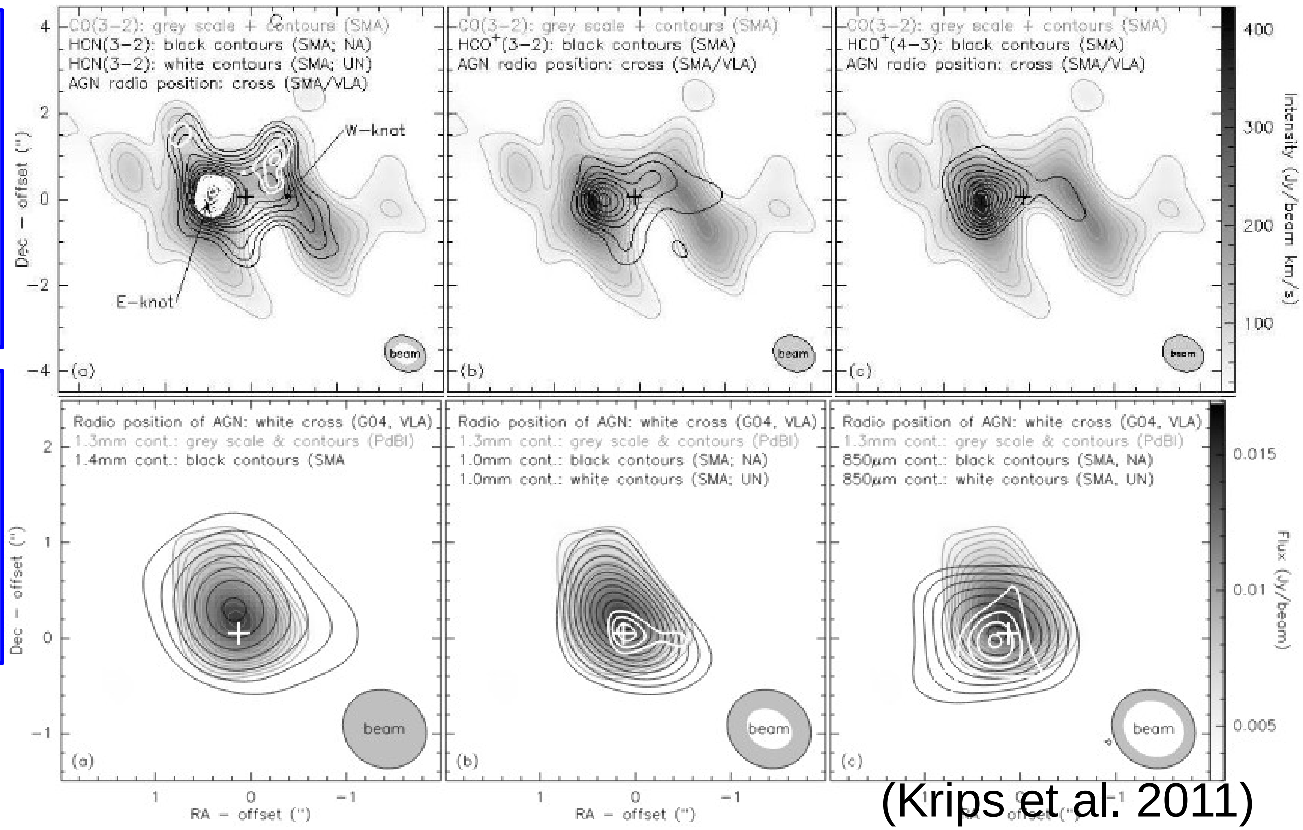

(Krips et al. 2011)

ALMA observations of NGC1068

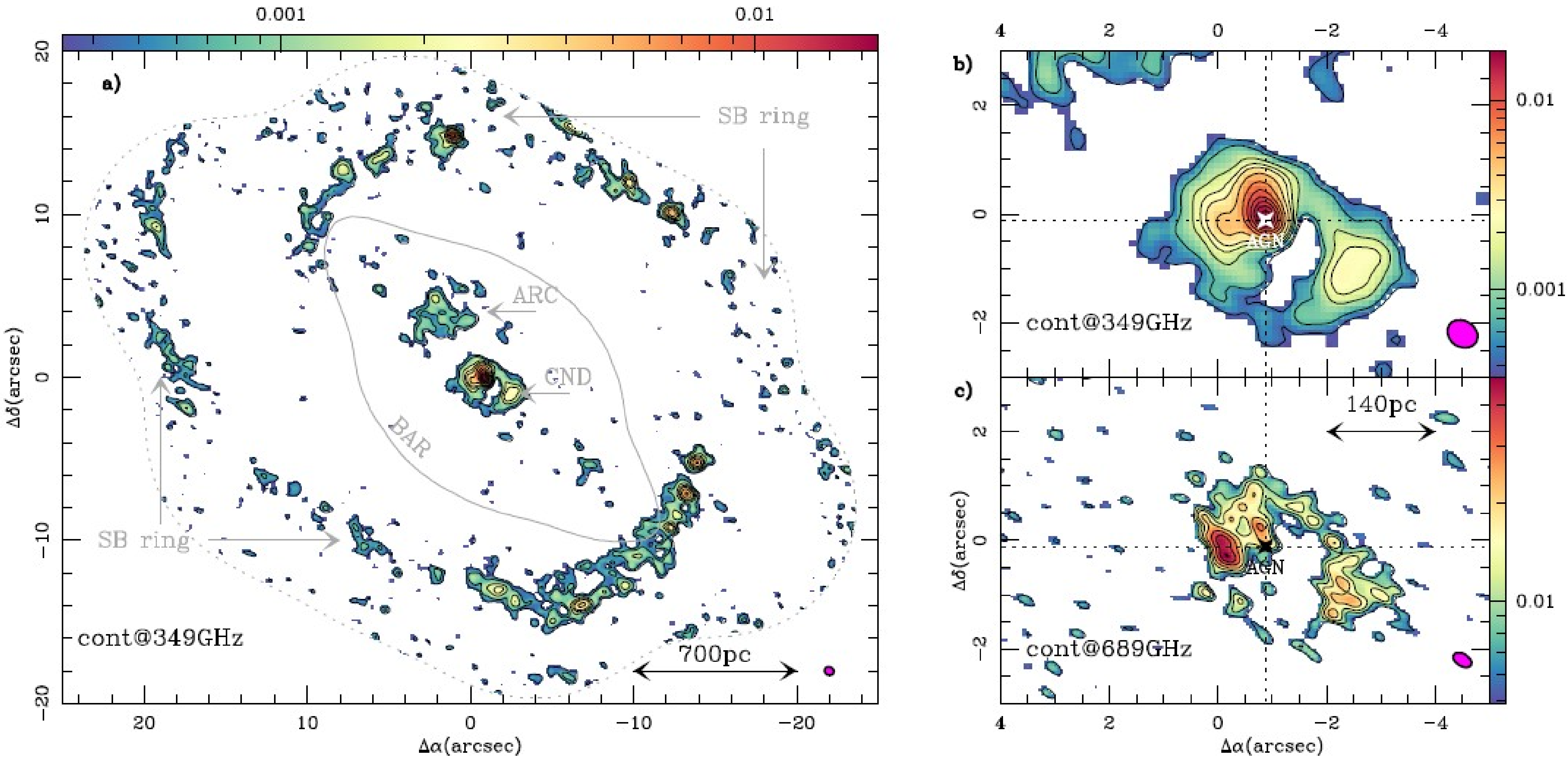

Continuum at 350 GHz: peak on AGN, off-centered ring around AGN
Spiral starburst ring at r=1.3 kpc, strange arc NE of the circumnuclear disk,
Maybe associated to the shock from the jet.
From SED fitting: $M_{\mathrm{torus}} = 2.1(\pm 1.2)\times 10^5\, M_\odot$

ALMA observations of NGC1068

CO 3-2 & 6-5 Emission

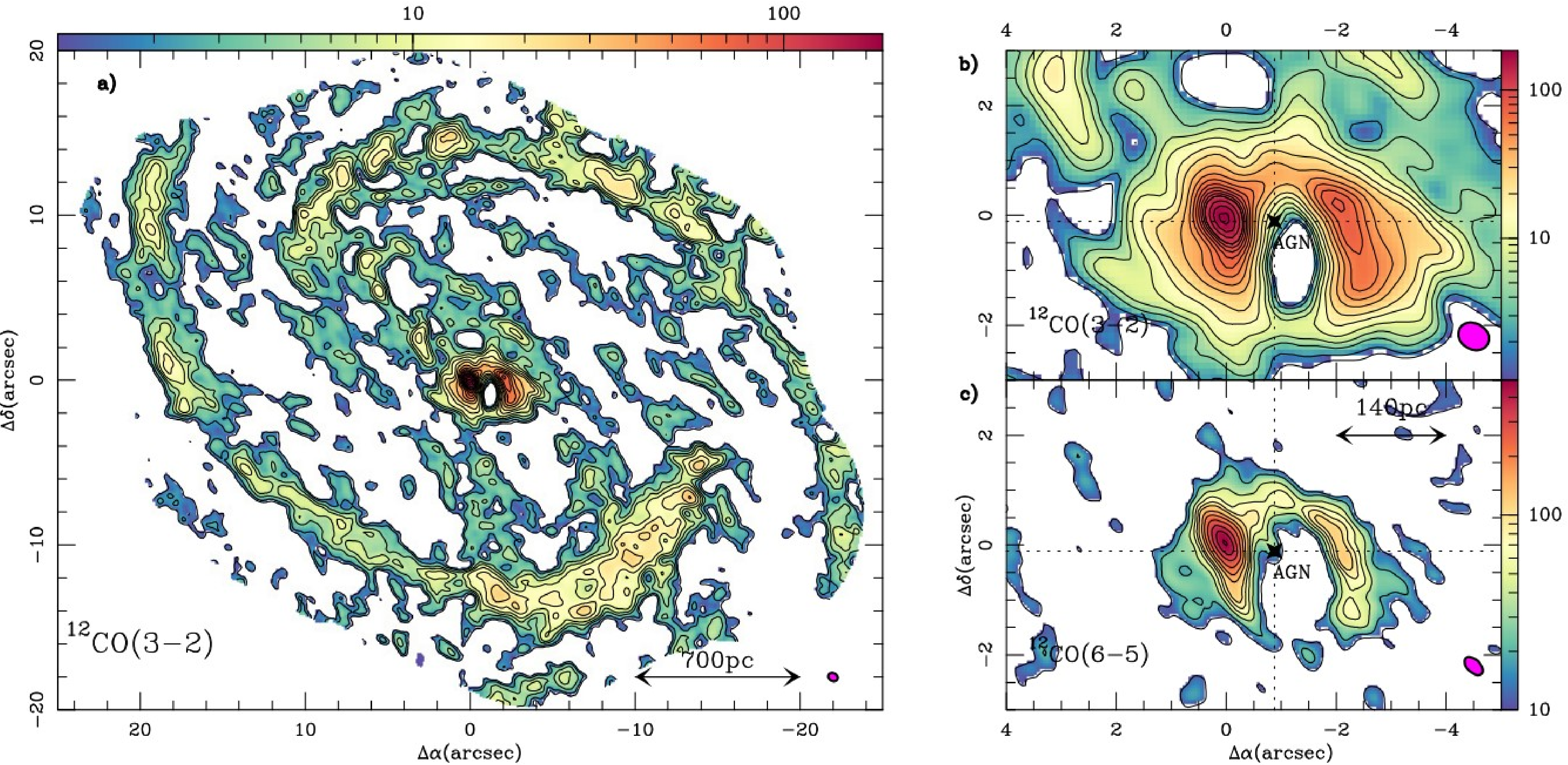

Molecular ring, CO does not peak on the AGN, large cavity cleared by AGN feedback.

ALMA observations of NGC1068

CO velocity field

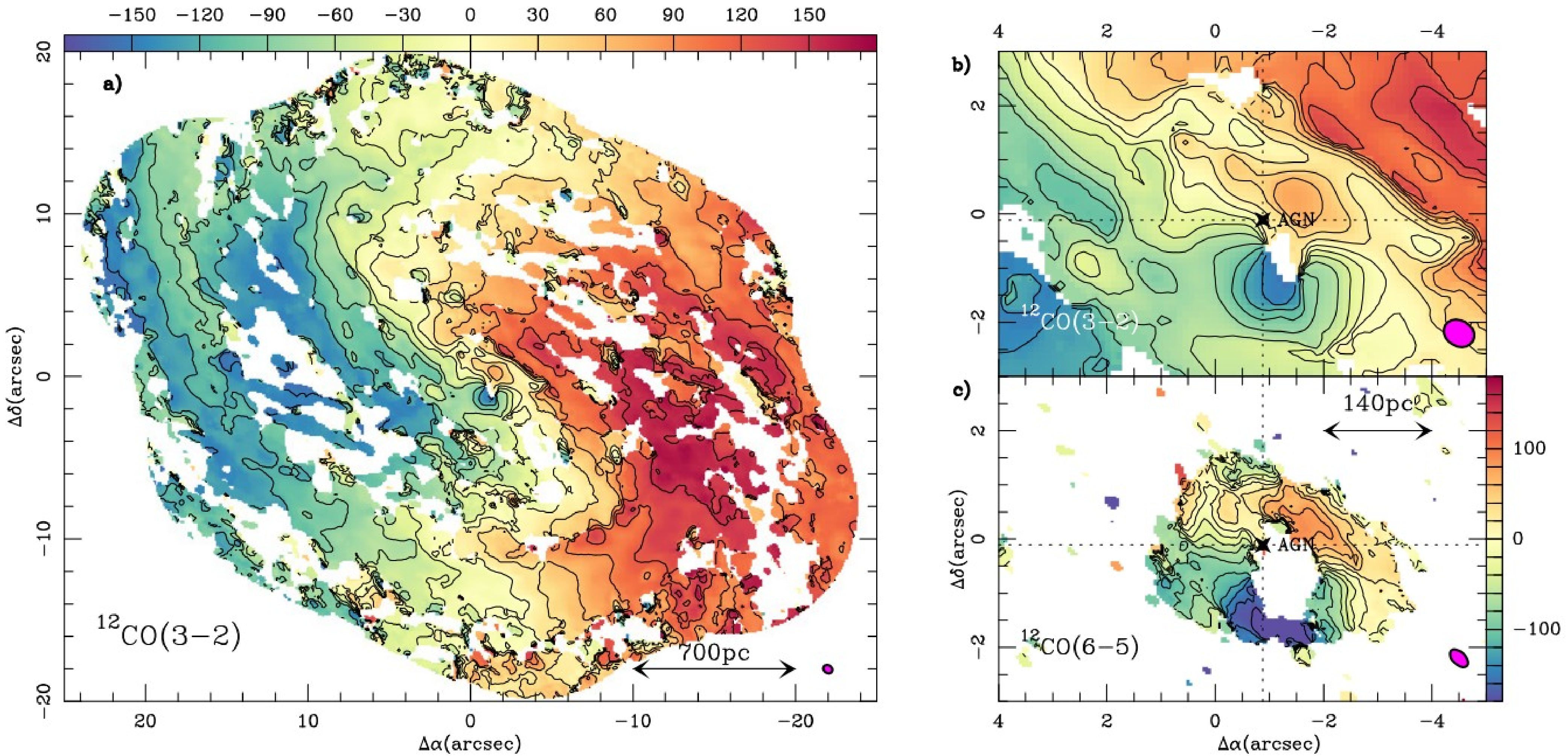

ALMA observations of NGC1068

CO velocity dispersion

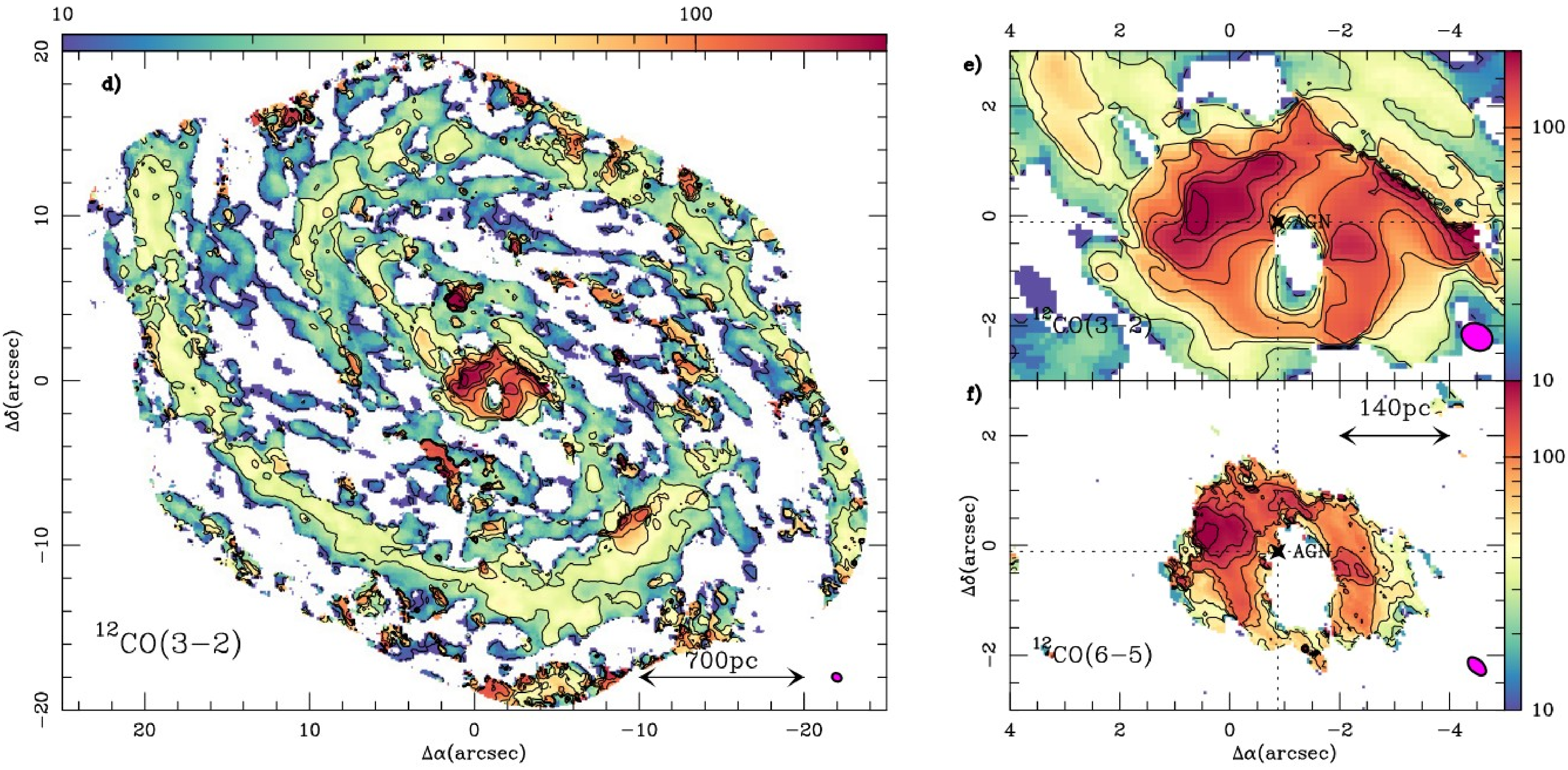

The velocity dispersion in the central 20 pc is 10^7 Msun, a good estimate of the SMBH mass

ALMA observations of NGC1068

The high resolution of ALMA and the high signal-to noise allow for a Fourier decomposition of the line of sight velocity , to look for non-circular motions

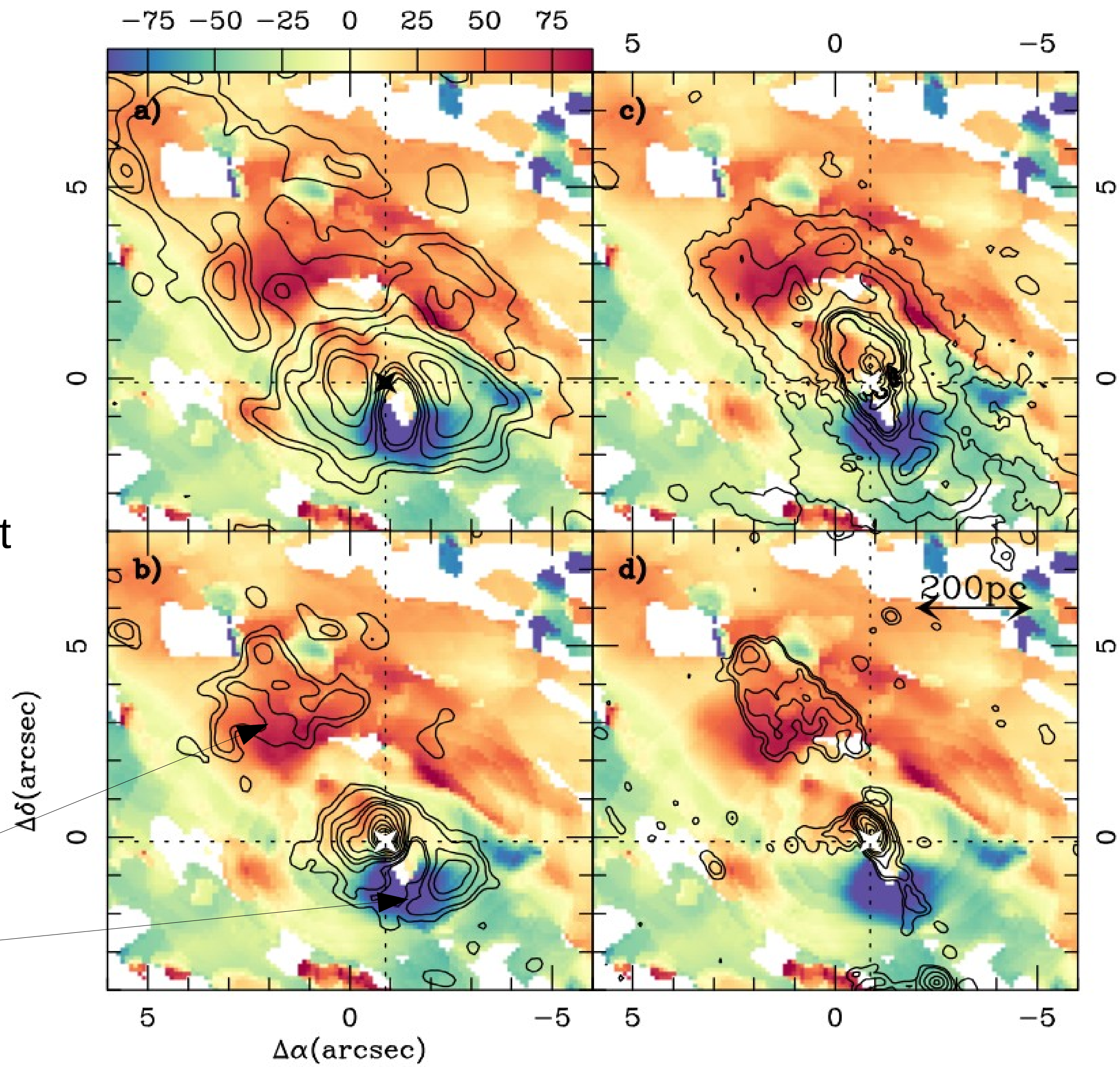

Color: Residual velocity field after Subtraction of rotational component

a) CO 3-2 integrated intensity

b) 349 GHz continuum

c) HST Pa emission

d) 22 GHz VLA map

Molecular outflow detected!

Red and Blue-shifted Outflow components!

ALMA observations of NGC1068

Mass outflow rate

$$\frac{dM}{dt} = 3 \times V_{\rm out} \times M_{\rm mol}/R_{\rm out} \times \tan(\alpha). = 63 \text{ Msun yr^-1 !}$$

From Infrared and K-band luminosity the star formation rate in the circumnuclear ring is SFR=1 Msun yr^-1

dM/dT >> SFR, outflow cannot be driven by star formation!

For a total gas mass of 10^7 Msun in the ring, the central starburst would run out of fuel in less than 0.2 Myr!

The outflow energetics are consistent with an outflow driven by radiation pressure fromthe AGN

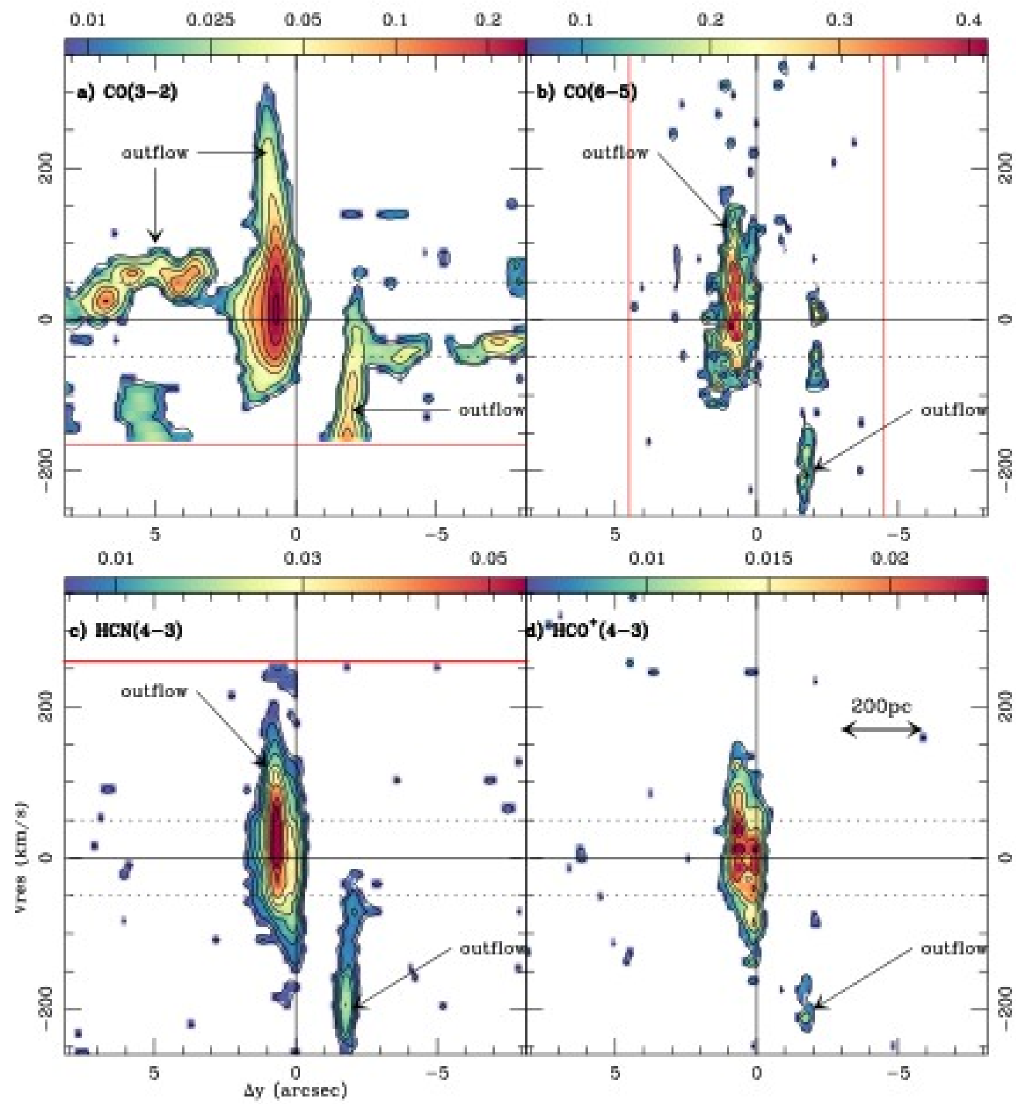

HCN/HCO+ ratio

In highly obscured AGNs the only radiation escaping the dust is the radio and mm-wave emission .
Molecular diagnostics is needed to detect hidden AGN.

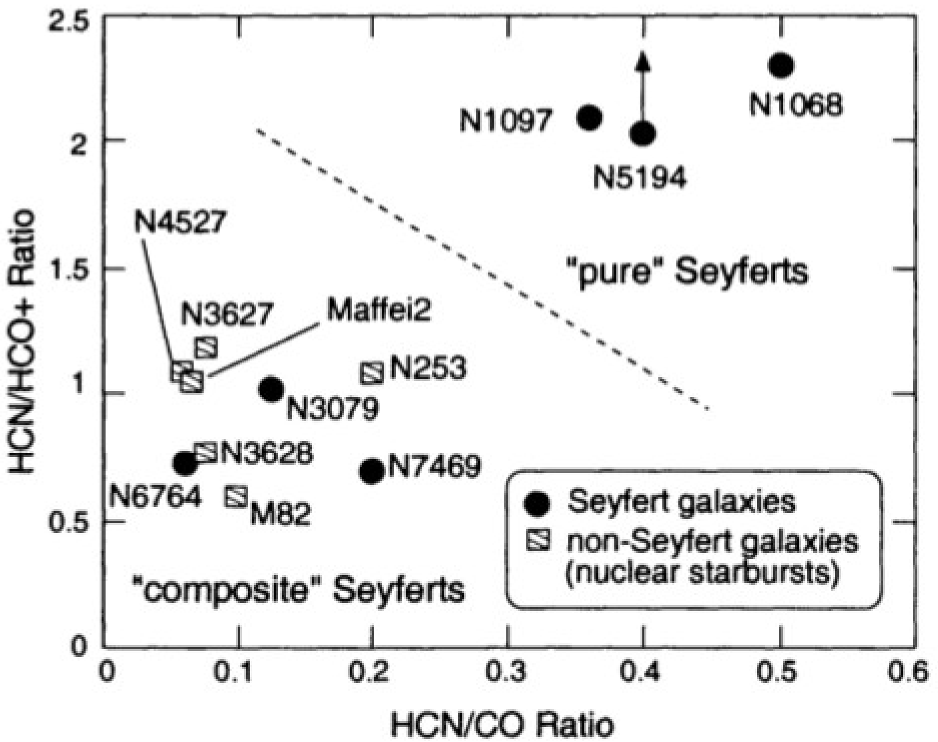

Kohno 2001

A suggested AGN tracer is the HCN/HCO+ Ratio, which is observed to be high in Seyferts And low in starbursts

This is usually explained with an X-ray Dominated chemistry around the AGN

However, theoretical explanations are very Controversial

Can this be used as an AGN tracer in highly obscured objects, where there may be little additional information ??

ALMA observations of NGC1068

High-density tracers: n>10^5 cm^-3

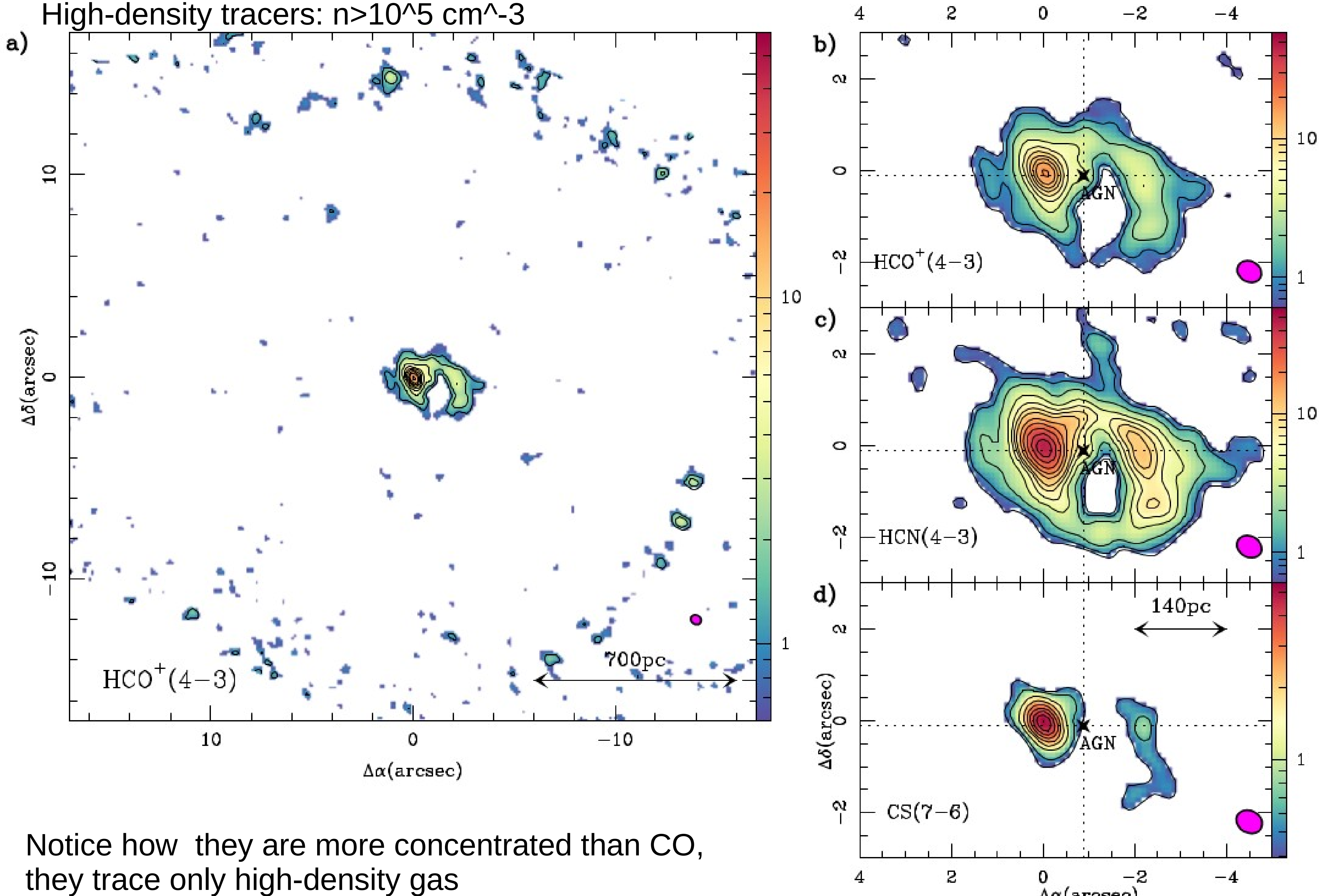

Notice how they are more concentrated than CO, they trace only high-density gas

Line ratios

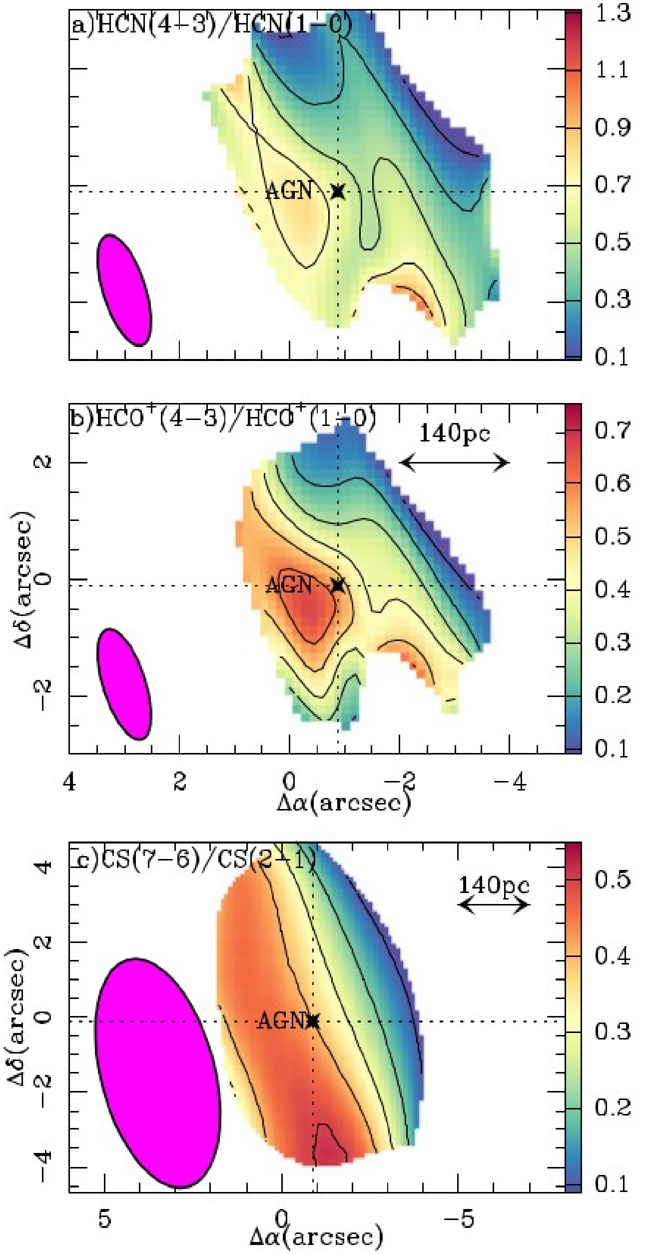

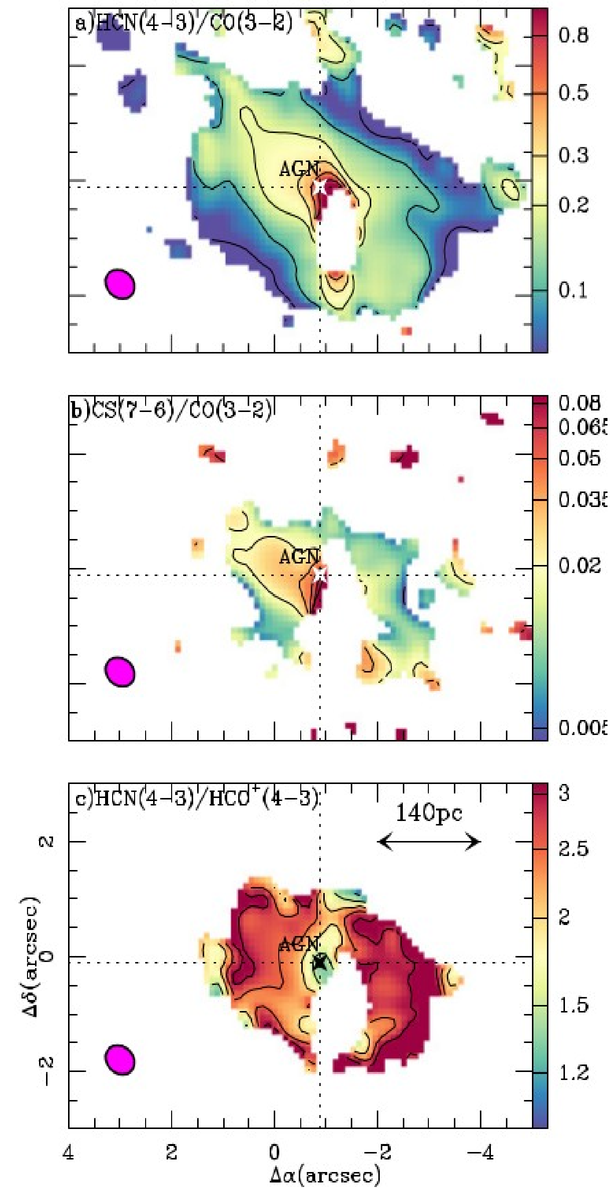

Line ratios of transitions with different critical density and excitation temperature: Density and Temperature gradients

Line ratios of different species with similar Excitation properties: Chemical differentiation

HCN/HCO+ ratio in NGC1068

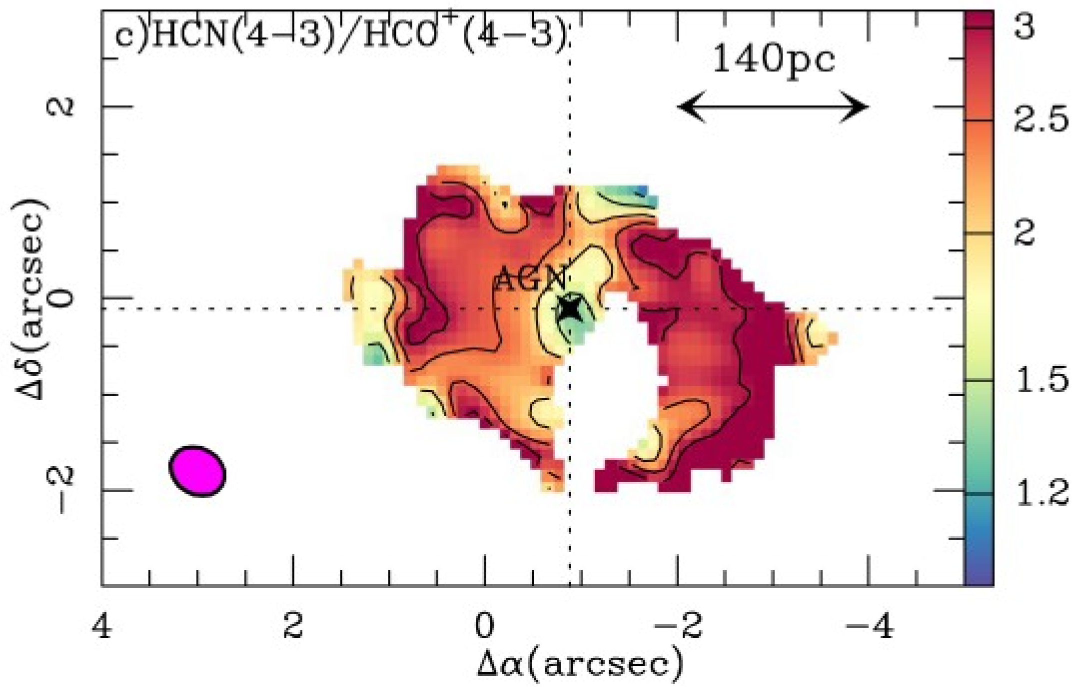

The HCN/HCO+ ratio is high in the circumnuclear disk, but lower at the position of the AGN.

The HCN/HCO+ ratio is not driven by X-ray dominated chemistry but probably by shocks from the AGN feedback.

Such a discovery has been made possible by the high resolution of ALMA, which can resolve the 20pc region around the AGN.

The PKS 1830-211 system

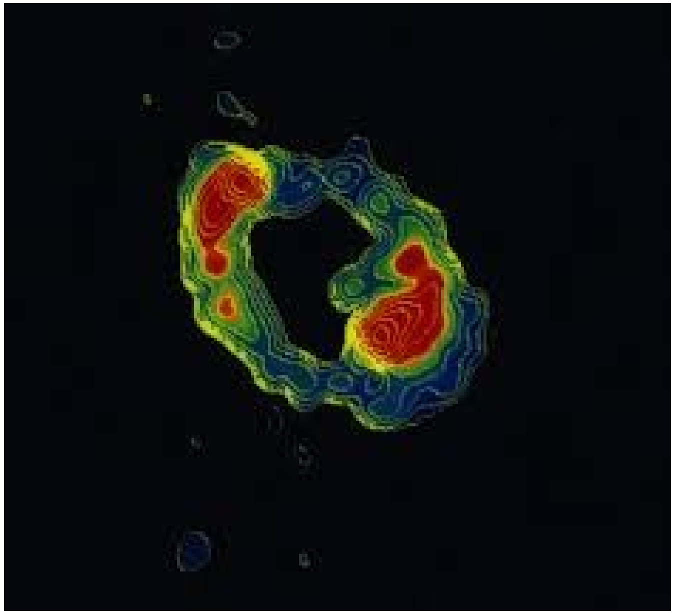

PKS1830-211 is a lensed system composed by
- a blazar at z=2.5
- a face-on spiral galaxy at z=0.89

The lensed image is splitted into two compact cores separated by ~1' and embedded in a fainter pseudo-Einstein ring

First double lensed quasar discovered (1929)

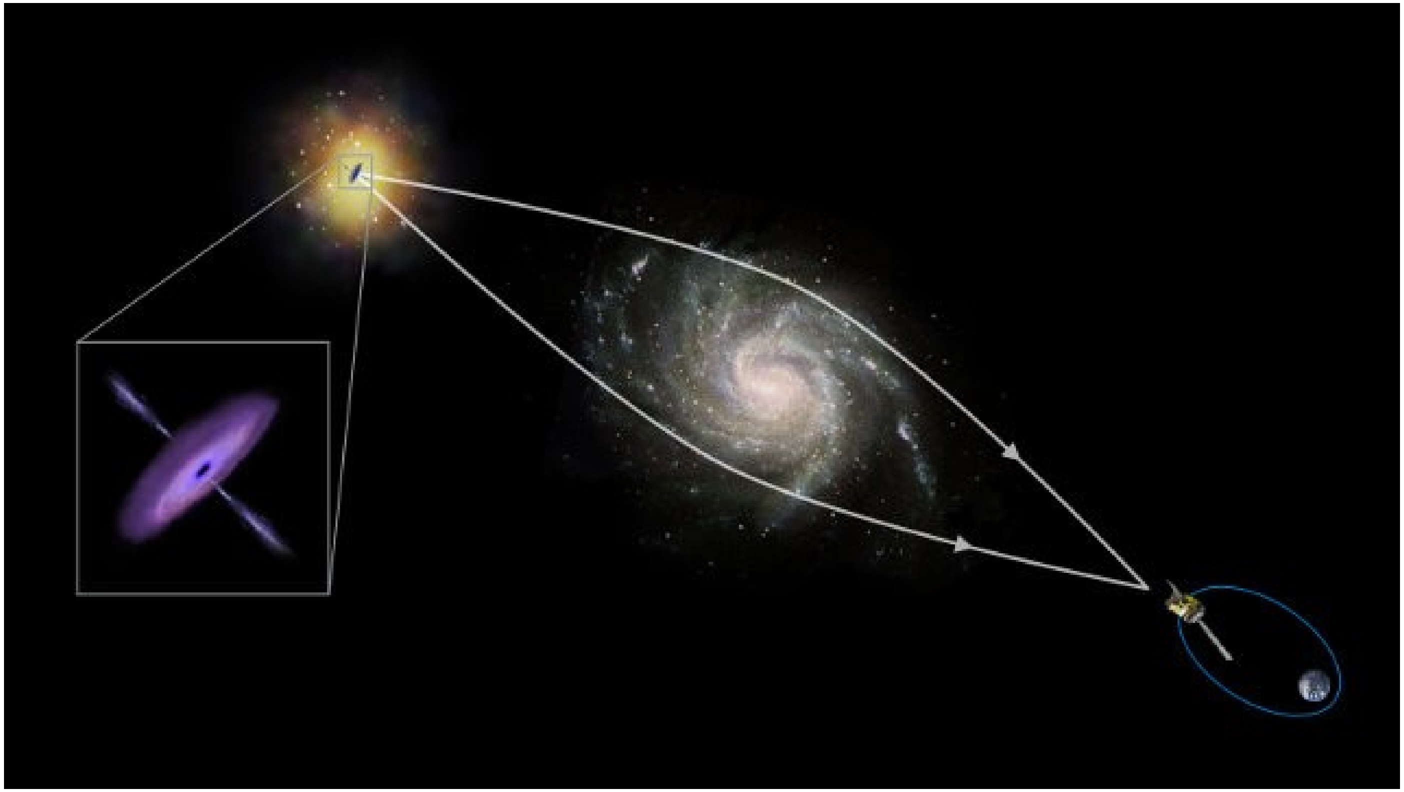

Absorption lines

Since absorption signal is not diluted by distance, the sensitivity is only limited by the brightness of the background continuum source, allowing even rare molecular species to be detected

At intermediate to high redshifts, molecules can serve as interesting cosmological probes. For example, the evolution of the temperature of the cosmic microwave background (CMB) has been investigated up to $z \sim 3$ using UV-band CO absorption-line systems observed in quasar spectra.

Mueller et al. (2013) have obtained a precise and accurate measurement of the CMB temperature, TCMB=5.08±0.10K at z=0.89 based on a multi-transition excitation analysis of a set of different molecular species seen in absorption toward PKS 1830−211 with ATCA. This value is fully consistent with the value TCMB=2.725 Kx(1+z)=5.14 K at z=0.89, yielded by adiabatic expansion of the Universe

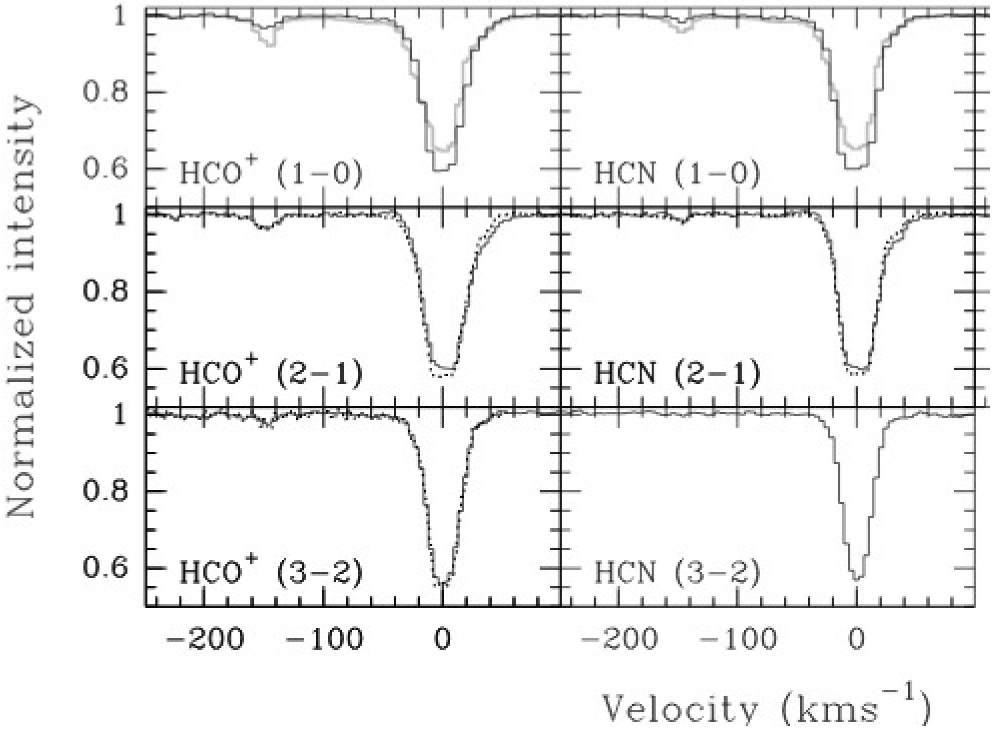

A survey of absorption lines towards PKS1830-211

(Mueller et al. 2014)

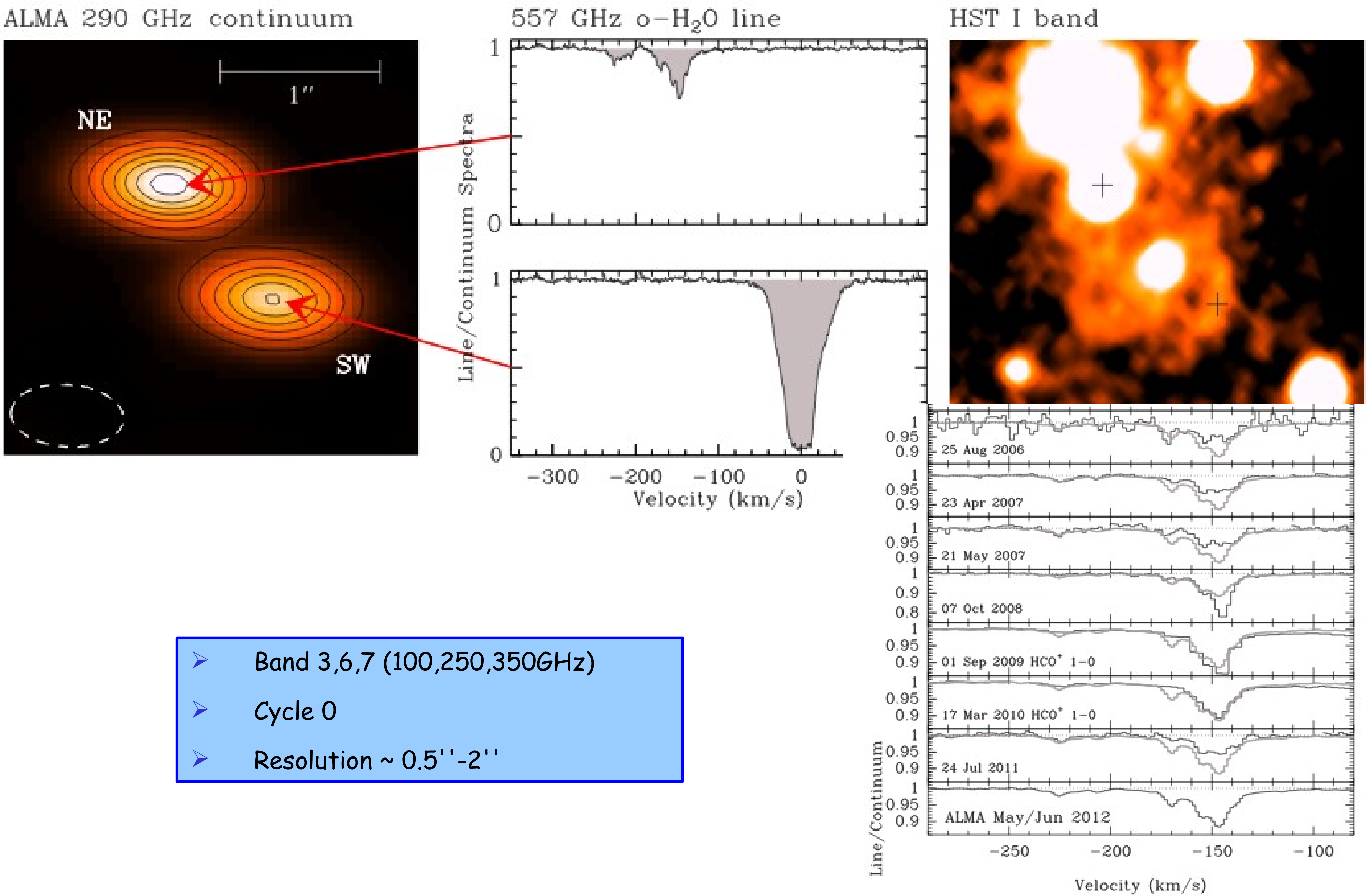

- Band 3,6,7 (100,250,350GHz)
- Cycle 0
- Resolution ~ 0.5''-2''

A survey of absorption lines towards PKS1830-211

(Mueller et al. 2014)

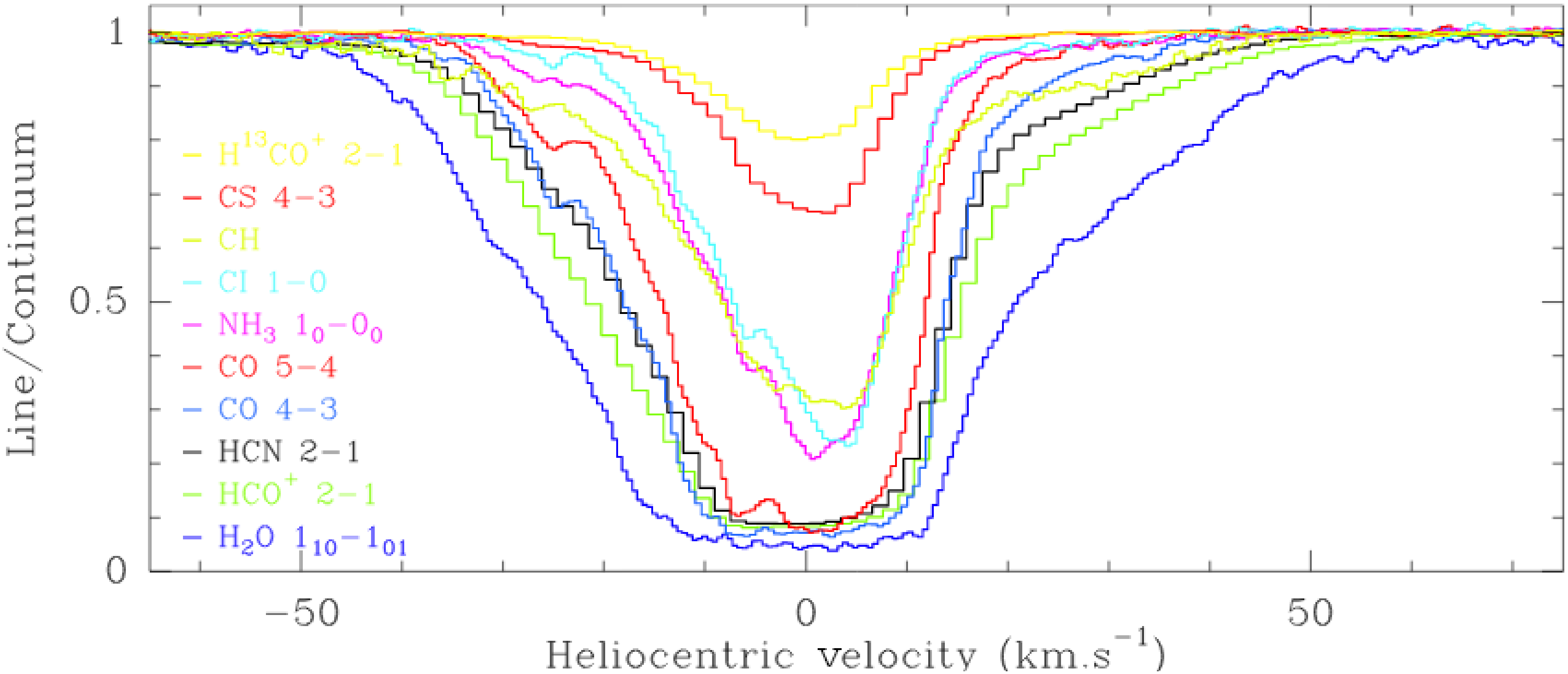

Toward the SW image	
1 atom	$H^{(d)}$, $C^{(in)}$
2 atoms	$\mathbf{CH}^{(n)}$, $OH^{(d)}$, $CO^{(bcin)}$, $^{13}\mathbf{CO}^{(n)}$, $CS^{(afn)}$, $C^{34}S^{(f)}$, $SiO^{(jkmn)}$, $^{29}SiO^{(kn)}$, $^{30}SiO^{(m)}$, $NS^{(k)}$, $SO^{(kmn)}$, $SO^{+\,(k)}$
3 atoms	$\underline{\mathbf{NH_2}}^{(n)}$, $H_2O^{(hn)}$, $\mathbf{H_2^{17}O}^{(n)}$, $C_2H^{(ekmn)}$, $HCN^{(aefkmn)}$, $H^{13}CN^{(efkmn)}$, $HC^{15}N^{(fkmn)}$, $HNC^{(aefkn)}$, $HN^{13}C^{(efkmn)}$, $H^{15}\overline{NC}^{(fkmn)}$, $N_2H^{+\,(ak)}$, $HCO^{+\,(aefkmn)}$, $H^{13}CO^{+\,(aefkmn)}$, $HC^{18}O^{+\,(fkn)}$, $HC^{17}O^{+\,(fkmn)}$, $HCO^{(kmn)}$, $HOC^{+\,(kmn)}$, $H_2S^{(f)}$, $H_2^{34}S^{(f)}$, $\underline{\mathbf{H_2Cl^+}}^{(n)}$, $\overline{\mathbf{H_2^{37}Cl^+}}^{(n)}$, $HCS^{+\,(m)}$, $C_2S^{(k)}$
4 atoms	$NH_3^{(ghn)}$, $H_2CO^{(cek)}$, $l\text{-}C_3H^{(k)}$, $HNCO^{(kn)}$, $\overline{HOCO^{+\,(m)}}$, $H_2CS^{(k)}$
5 atoms	$CH_2NH^{(kmn)}$, $c\text{-}C_3H_2^{(ekn)}$, $l\text{-}C_3H_2^{(k)}$, $H_2CCN^{(k)}$, $H_2CCO^{(k)}$, $C_4H^{(k)}$, $HC_3N^{(ejkn)}$
6 atoms	$CH_3OH^{(kln)}$, $CH_3CN^{(kn)}$, $NH_2CHO^{(m)}$
7 atoms	$CH_3NH_2^{(kn)}$, $CH_3C_2H^{(kn)}$, $CH_3CHO^{(k)}$
Toward the NE image	
1 atom	$H^{(d)}$, $\mathbf{C}^{(n)}$
2 atoms	$\mathbf{CH}^{(n)}$, $OH^{(d)}$, $\mathbf{CO}^{(n)}$
3 atoms	$\mathbf{H_2O}^{(n)}$, $C_2H^{(kn)}$, $HCN^{(fkmn)}$, $HNC^{(fk)}$, $HCO^{+\,(cfkmn)}$, $\underline{\mathbf{H_2Cl^+}}^{(n)}$
4 atoms	$\mathbf{NH_3}^{(n)}$, $H_2CO^{(k)}$
5 atoms	$c\text{-}C_3H_2^{(k)}$

A strong magnetic field in the jet base of a SMBH

(Marti-Vidal et al. 2015)

Studying the polarization of the nonthermal emission from AGN is a direct way to probe the structure and strength of magnetic fields in the vicinity of a black hole.

→ importance of the observation of RM, defined as the change of polarization angle as a function of wavelength squared. RM ~ to the plasma density and the strength of the magnetic field along the line of sight.

To date, it has been extremely difficult to obtain accurate polarimetric information from the innermost (subparsec) regions of AGN; only emission at submillimeter wavelengths can escape from these regions, due to a large synchrotron self-absorption that blocks the emission at longer wavelengths.

XX, YY, and YY-XX polarization images

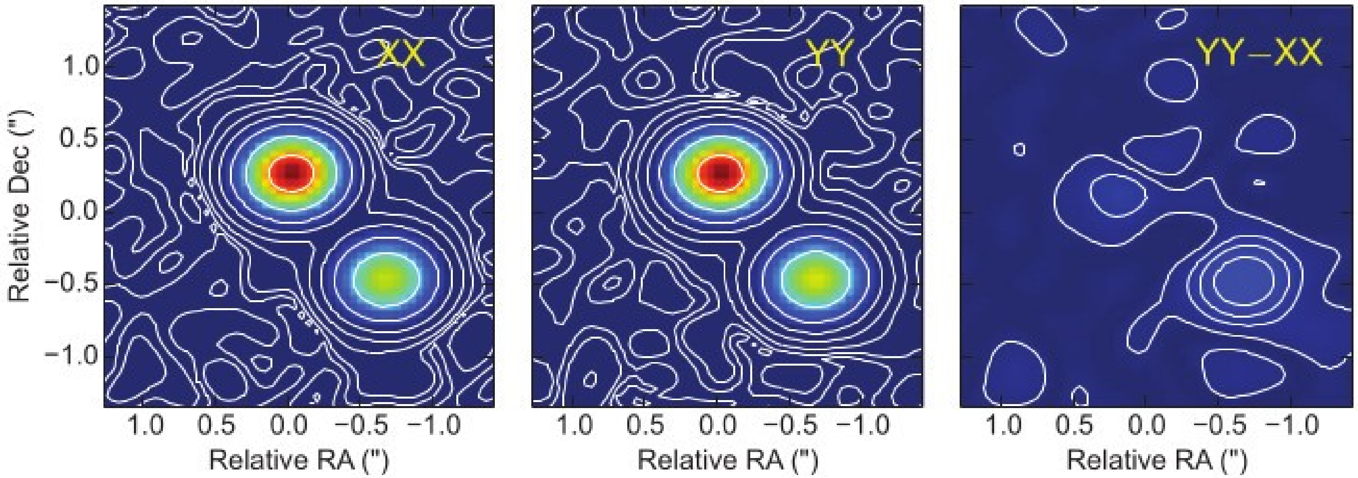

Detection possible thanks to the high resolution (sub-arcsec) and to the use of a new differential polarimetry technique (see after).

A strong magnetic field in the jet base of a SMBH

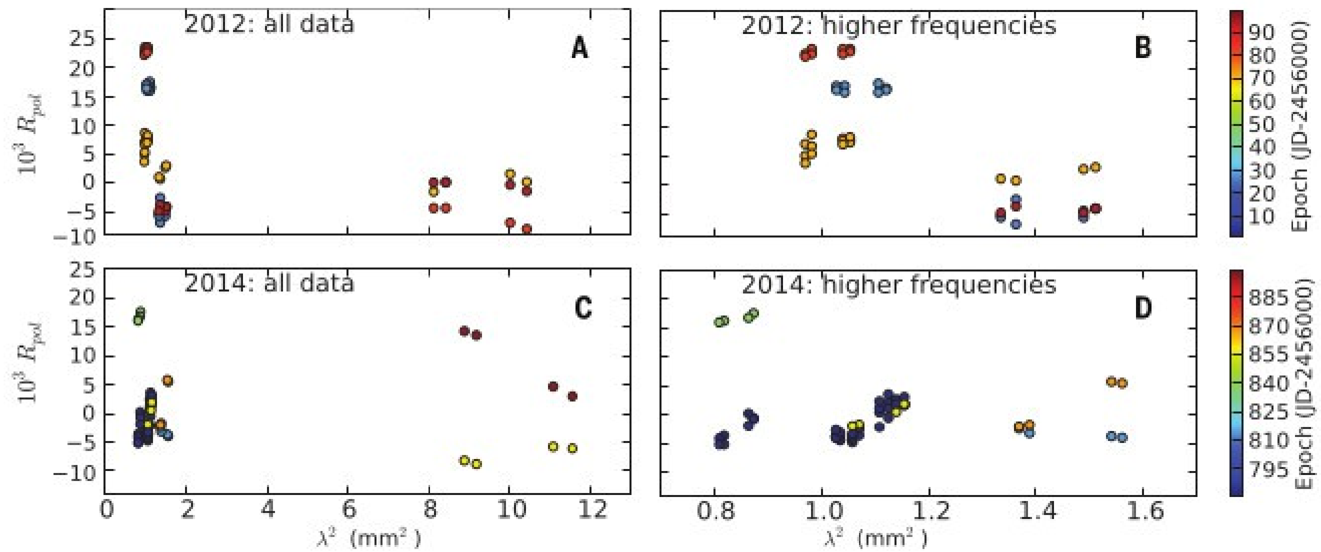

Large variations of RM with wavelength cannot be explained if the RM is only caused by an external (e.g., spherically symmetric) **screen** of material being accreted onto the black hole] and/or by external clouds. would be similar for all the submm jet emission.

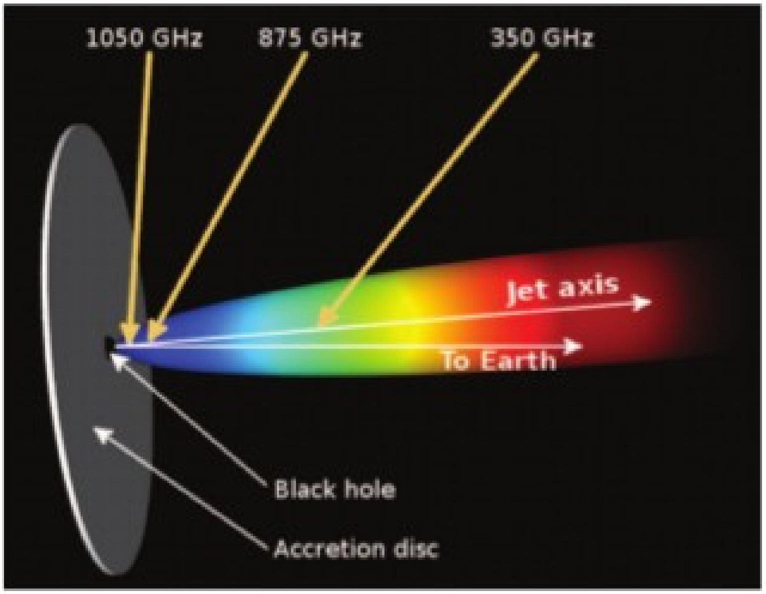

The Faraday screen must thus be close to the jet base and change substantially on sub-parsec scales.
An increase of the RM at shorter wavelengths would then be explained naturally as an increase of the magnetic field strength and/or electron density as we approach the black hole.

Sketch of the jet launch/acceleration region in PKS 1830−211 (not to scale). Emission at higher frequencies comes from material closer to the black hole, at subparsec scales. At these frequencies, the main contribution to RM must come from a zone close to the jet, in order to explain the different RM values between 350 GHz and 0.8 to 1 THz (source frame).

A strong magnetic field in the jet base of a SMBH

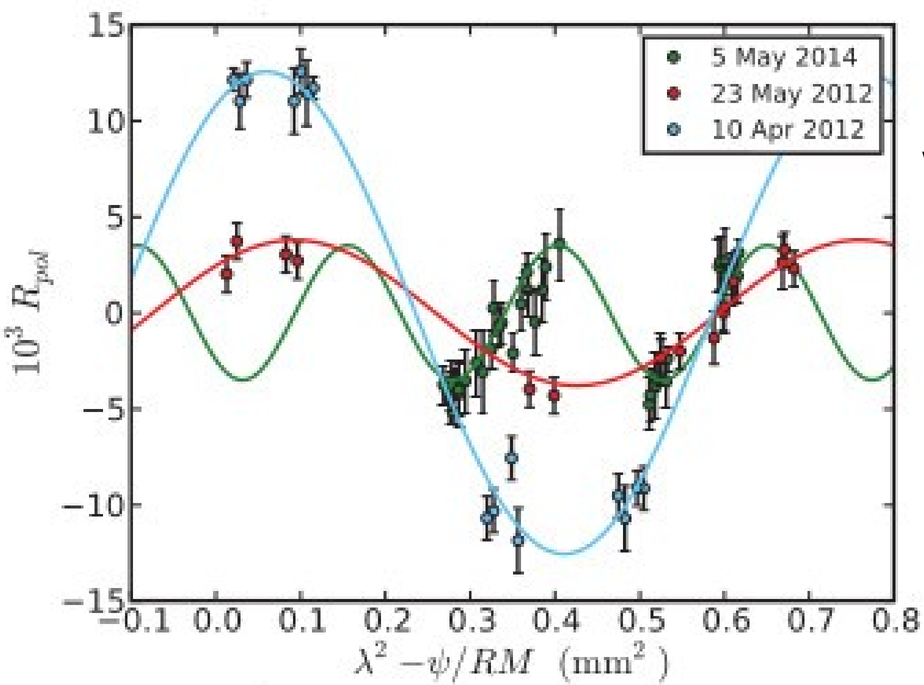

2012 obs. taken before and after a **gamma-ray flare**. 2014 data coincident to an other gamma-ray flare which had a strong radio counterpart, and it may also be related to the higher RM measured in 2014.

The high variability in RM, in connection to the gamma-ray flaring events, points toward a **cospatial origin of the gamma-ray emission** and the 250- to 300-GHz RM, hence favoring the interpretation of the RM being caused at the region very close to the jet base.

RM will be an important test for detailed magnetohydrodynamical (MHD) models at the jet base.
The rotation measures derived here, RM ~ 10^8 rad/m^2 in the rest frame of the source, are about a factor of 10^5 greater than the rest-frame RM values measured for parsec-scale AGN cores, where the derived magnetic fields have been independently measured to be ~0.05 to 0.10 G
Hence, there are very high magnetic fields at the jet base, which should be **dynamically important near the black hole and should in turn affect the accretion process.**

Observations in highly obscured galactic cores

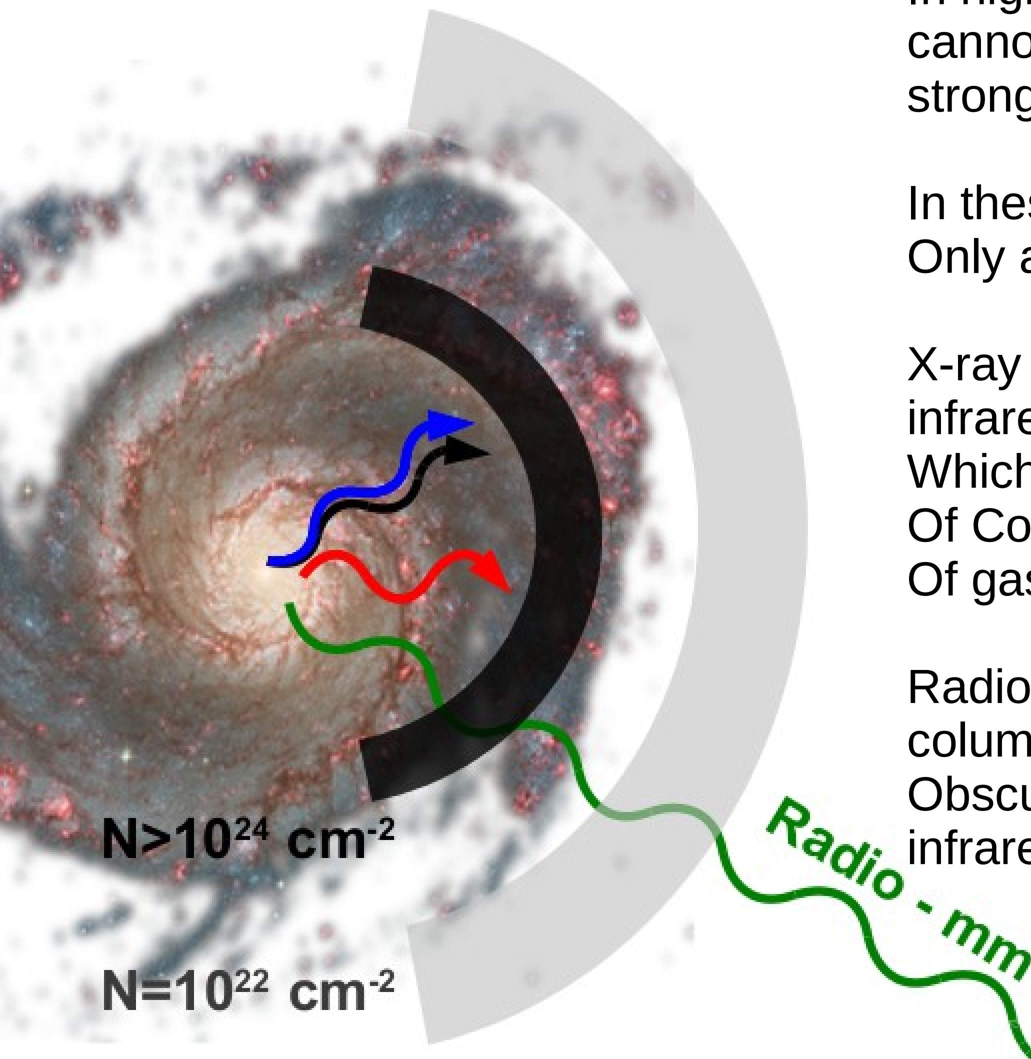

In highly obscured systems, optical observations cannot probe the nuclei of galaxies because of strong absorption by dust

In these systems, IR radiation is optically thick and Only a featureless photosphere surrounds the nucleus

X-ray surveys reveal that most luminous infrared galaxies host highly obscured AGN, Which are undetectable even in X-rays because Of Compton losses due to the high column density Of gas and dust along the line of sight

Radio and mm-wave radiation can penetrate large columns of dust and gas and is the only tracer of the Obscured regions of compact luminous infrared galaxies

ALMA reveals a chemically evolved SMG at z = 4.76

PI: C. De Breuck

PI: R. Gilli

LESS J033229.4-275619

Nagao et al. 2012

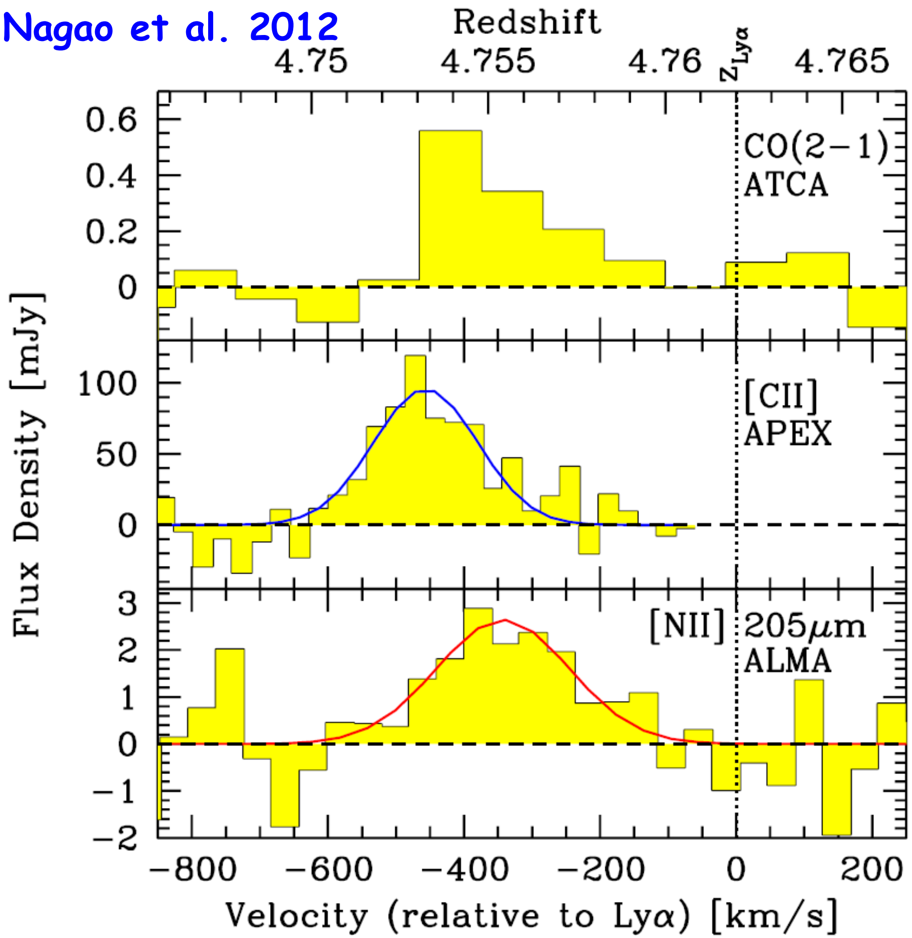

Band 6, 250 GHz, 18 antennas, 3.6 hrs, 1.5" res (PI: Nagao)

[NII] 205 μm detection: [NII] arises from HII regions (Nagao et al 2011)

The first measure of [NII]/[CII] in high-z galaxies, ~0.043, similar to the nearby Universe

[NII]/[CII] metallicity indicator: as the metallicity in this SMG is consistent with solar, **the chemical evolution has progressed very rapidly**

Band 6, 1.3 mm continuum, 17 antennas, 23 min (including cal.), 0.75" res (PI: Gilli)

First measure of the dust temperature, Tdust ~ 60 K (with ALMA + Herschel), mass and size.

Warm and compact starburst surrounds an obscured BH. Progenitor of local compact quiescent galaxies

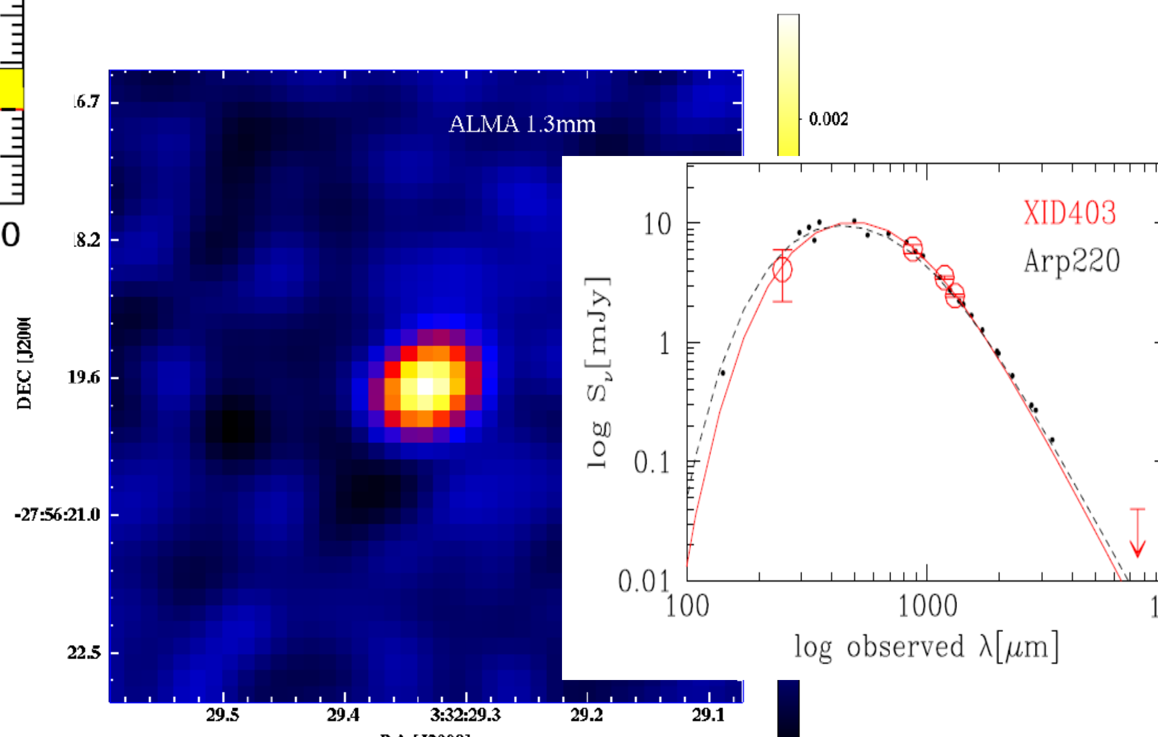

Gilli et al 2013 – Supported by Italian ARC

Cosmic Infrared Background

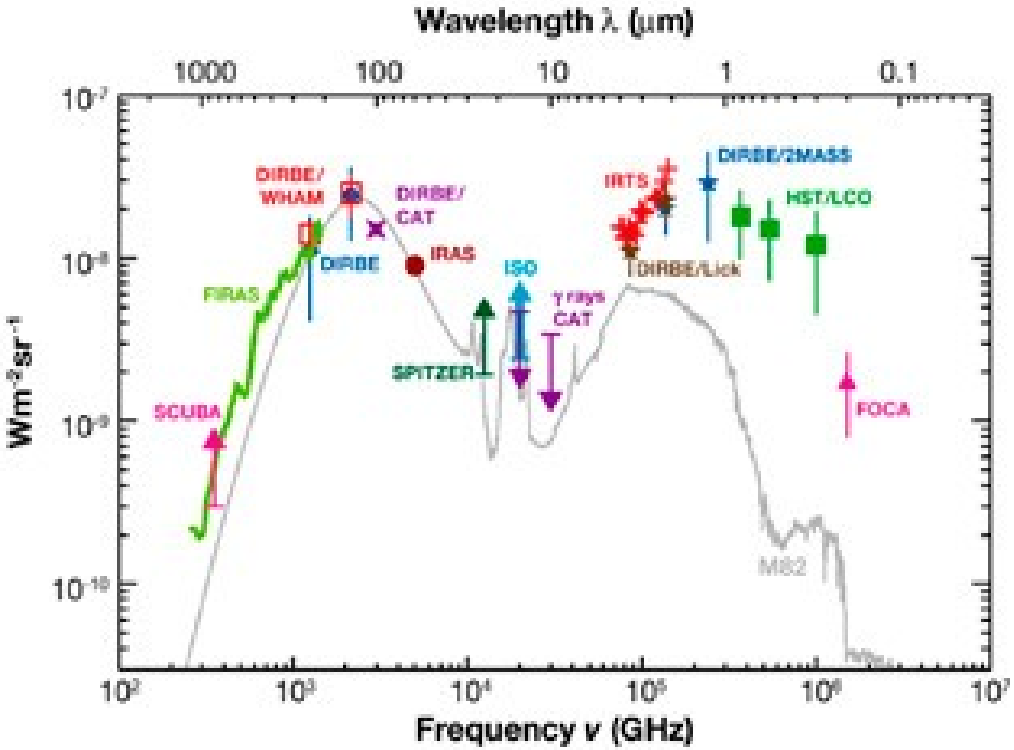

The power in the infrared is comparable to the power
in the optical.
Locally, the infrared output of galaxies is only one third of the optical output.

This implies that **infrared galaxies grow more luminous with increasing z faster than optical galaxies.**

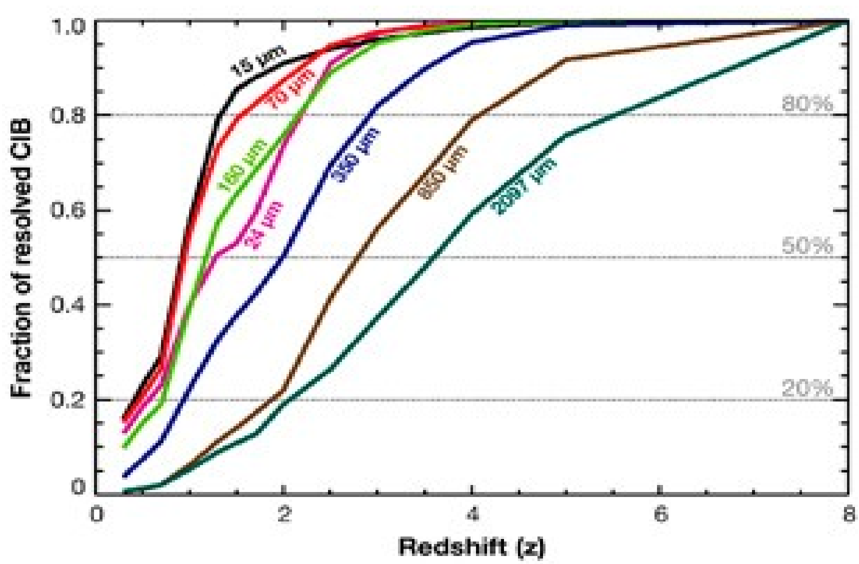

(Lagache et al. 2005)

The fraction of resolved CIB as a function of z.
50% of the CIB is due to galaxies at
z<1 at 15 and 70 μm,
z<1.3 at 24 and 160 μm,
z<2 at 350 μm,
z<3 at 850 μm
z<3.5 at 2 mm
The CIB at longer wavelengths
probes sources at higher redshifts.

(sub)mm galaxy populations

SCUBA surveys (Blain et al. 2000) identified the existence of **a population of highly dusty galaxies with high SFR.** Limits to their classification and observations were mostly due to confusion.
They were defined **SubMillimeter Galaxies (SMG)**.

CO observations (Genzel et al. 2003, Greve et al. 2005, Tacconi et al. 2008...) measured masses and redshift for the SMGs, observing that there is a large fraction of massive galaxies at **$z>2$**.

These fractions were at odds with hierarchical formation models
(larger galaxies are formed through the continuous merging of smaller ones)
and were the basics of "downsizing" (most massive galaxies form earlier and faster).

Chapman et al. (2003,2005) exploited the FIR-radio relation for SMGs to select them in radio bands and found that redshift distribution is similar to those of QSOs and that they contribute to SF history at z=2

In the FIR the dust is predominantly heated by the star-formation activity rather than by the AGN also in QSO (Beelen et al. 2004).

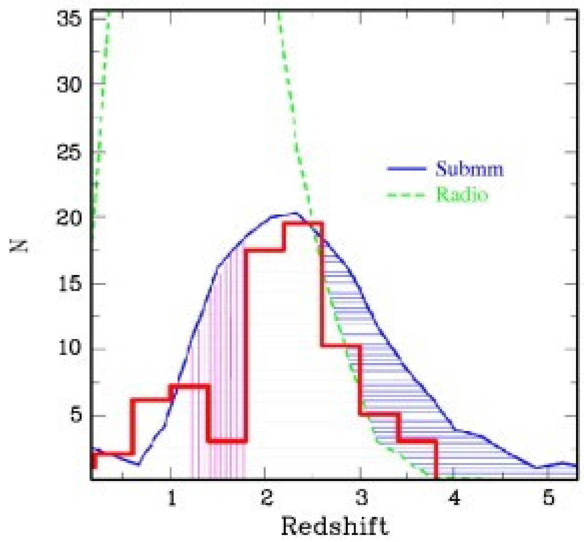

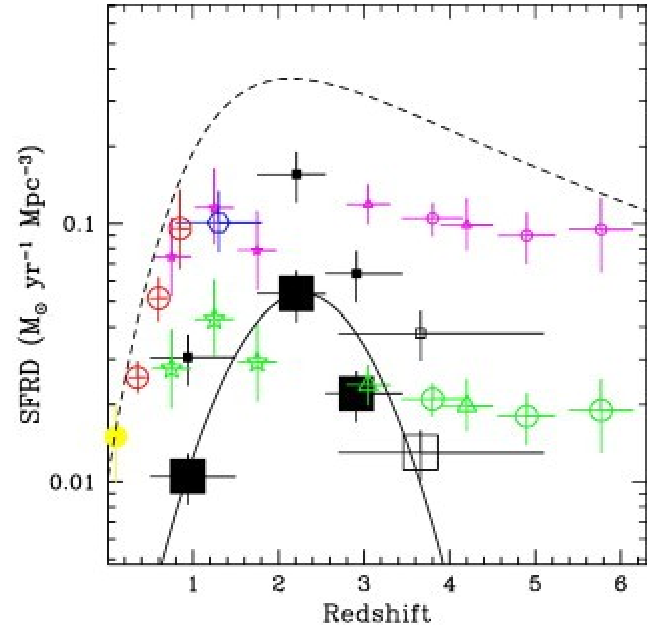

Example: Anti-hierarchical model

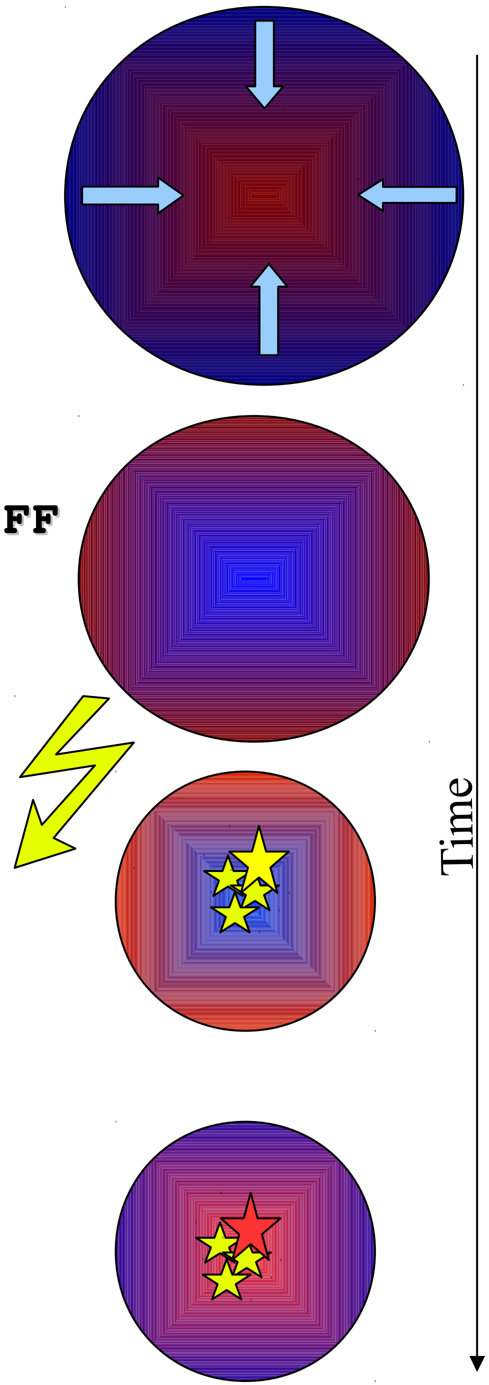

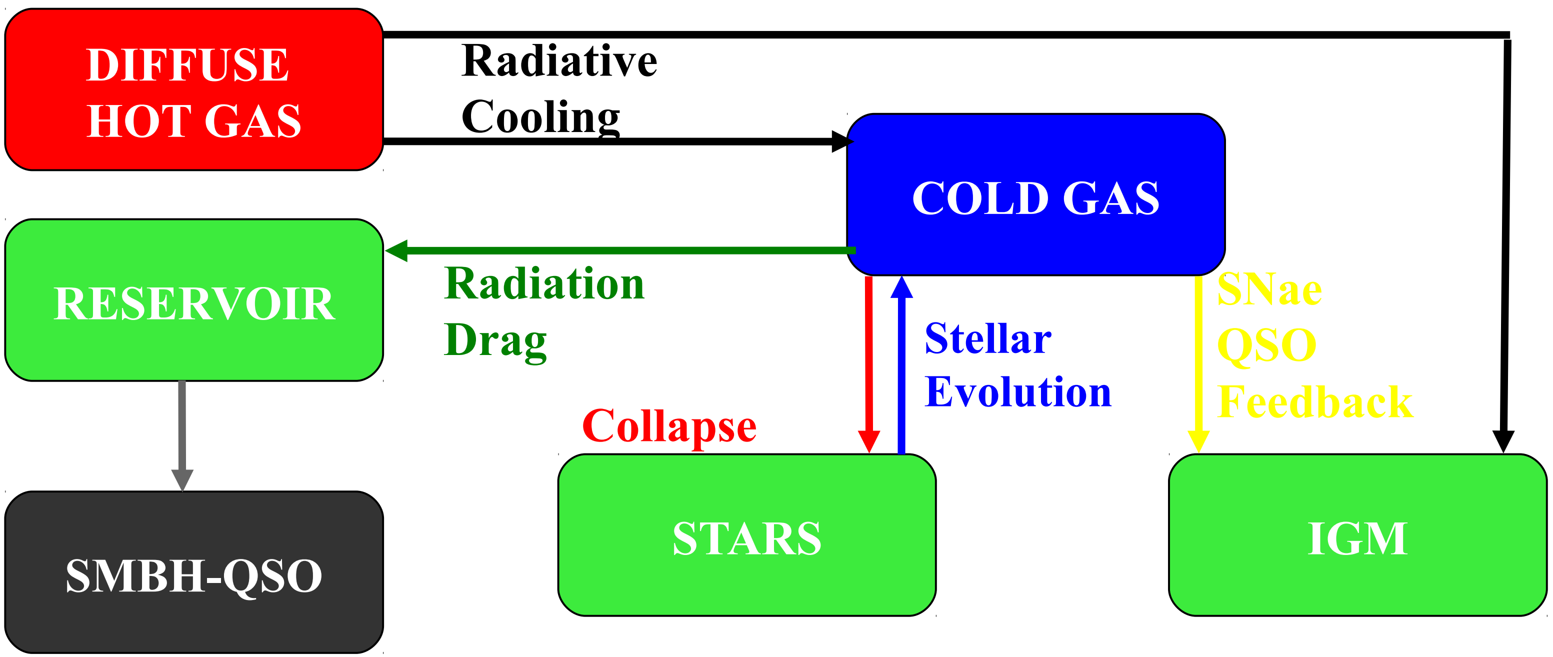

Virial Collapse : the gas becomes hotter and denser
Radiative cooling : free-free emission and SF
Radiation drag : reduces the gas angular momentum and produces a reservoir torus that feeds the central SMBH
SNae feedback : the gas is reheated and shocks are created, generating denser regions where SF continues
Most massive clouds have higher SFR and faster depletion time
AGN feedback: halts the collapse

Granato et al. 2004

(sub)mm galaxy populations

SMGs are the high redshift counterparts of local massive elliptical galaxies
(ULIRGs L_FIR>10^{12} L_sun),
with AGN activity obscured by the high dust content.

Open issues remain:
- What is the role of starburst or AGN activity in powering the dust heating and associated infrared emission?
- What is the role of merging events?
- What inject the SF events?

- Which are the properties of the dusty torus of AGN?
- How does the AGN feed the BH?
- How the AGN interact with the host galaxy?

- Which is the most probable evolutionary scenario?
- They are only the tip of the iceberg, how do 'normal galaxies' evolve?

...

Answers - in the (sub)mm signals
- matching low to high-z observations

An ALMA survey of submm in the Extended Chandra Deep Field South

PI: I. Smail

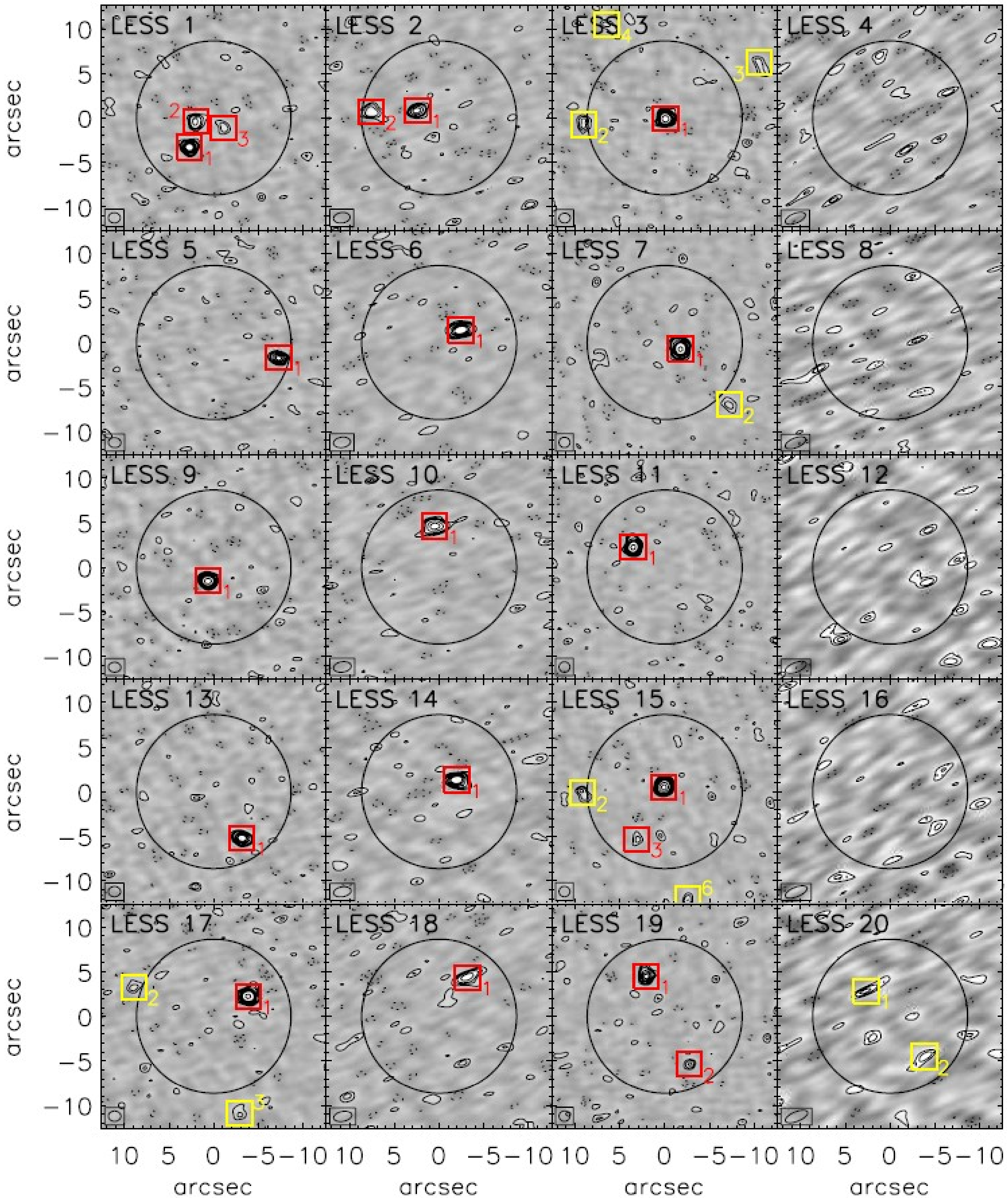

OBSERVATIONS

- 870 µm (Band 7) follow-up of a LABOCA Extended Chandra Deep Field South Submm Survey (LESS)
- **122 submm sources**
- ~15 antennas, FOV = 17", **2 min/source**
- rms < 0.6 mJy/beam (**x3 deeper than LABOCA**)
- Resolution ~1.5" (**x10 better than LABOCA**)

~35% of the detected LABOCA sources are resolved in multiple SMGs

In 2 SMGs detection of [CII] 158 **µ**m at z ~ 4.4: ALMA able to detect the dominant fine-structure cooling lines with short integration

Selections in radio/mid-IR bands miss 45% of SMGs

First statistically survey of SMGs: basis for an unbiased multifrequency study of SMGs

Median redshift of z_phot=2.5±0.2 with 35±5 per cent of SMGs lying at z >3

Hodge et al 2013; Karim et al. 2013; Simpson et al. 2013, Swinbank et al. 2014, and many other papers ….

An ALMA survey of submm in the Extended Chandra Deep Field South

PI: I. Smail

- By fitting and averaging the SEDs, the far-infrared luminosities are
  L_FIR=(3.0±0.3)×10^{12} L_sun (SFR=300±30 M_sun/yr)
- The characteristic dust temperature is Td=32±1 K
  (3–5 K lower than comparably luminous galaxies at z=0, reflecting the more extended star formation in these systems).

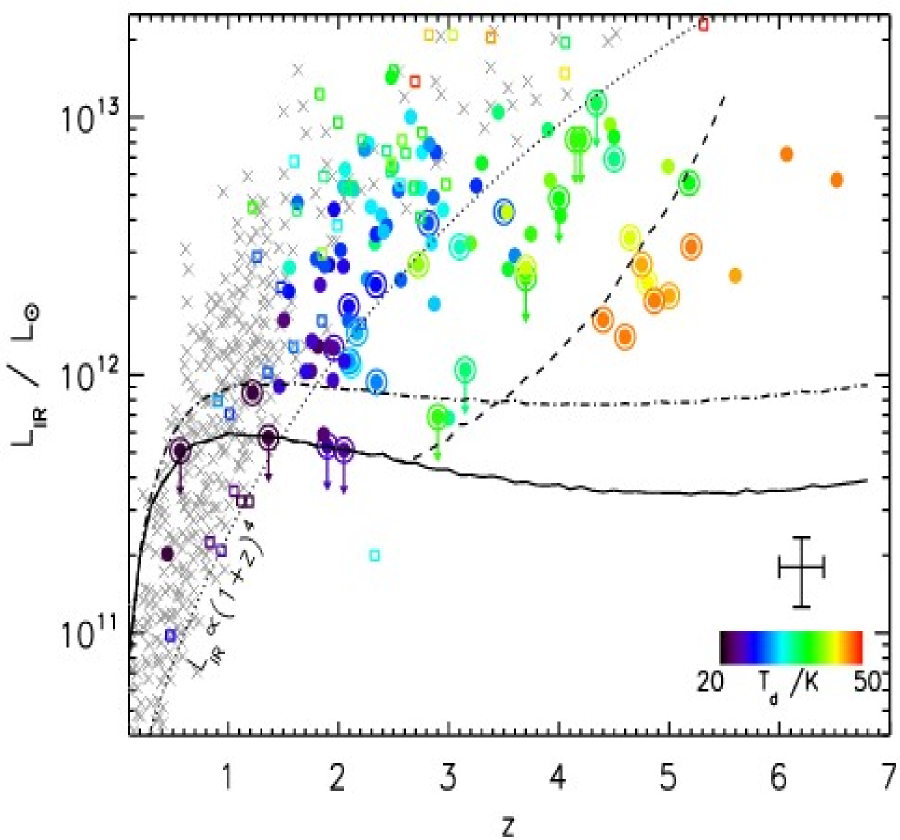

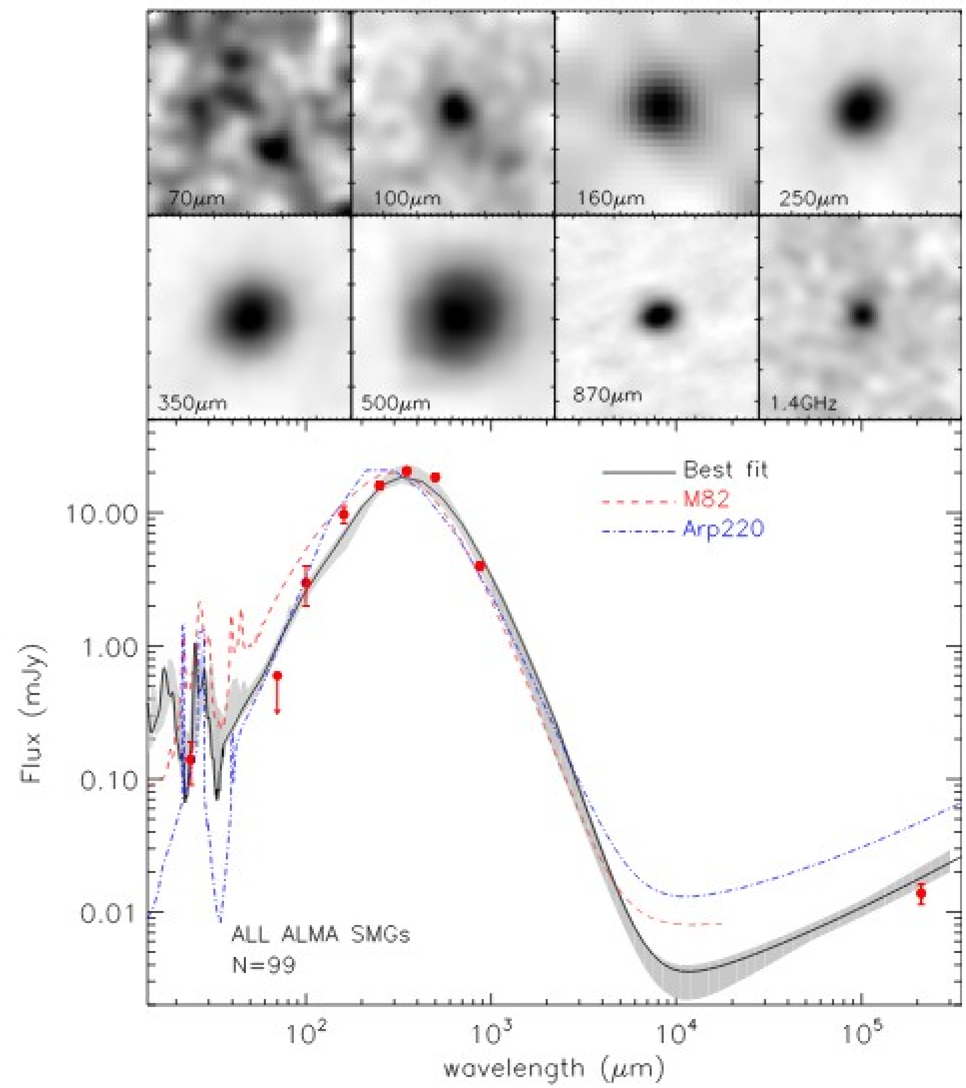

Swinbank et al. 2014

An ALMA survey of submm in the Extended Chandra Deep Field South

PI: I. Smail

- The contribution of S(870μm)≥1 mJy SMGs to the cosmic star formation budget is 20% of the total over the redshift range z∼1–4.
- Adopting an appropriate gas-to-dust ratio, the typical molecular mass of the SMGs is $M(H_2)=(4.2\pm0.4)\times10^{10} M_{sun}$
- SMGs with S(870μm)>1mJy ($L_{FIR}>10^{12} L_{sun}$) contain ∼10 per cent of the z∼2 volume-averaged H2 mass density
- Redshift distribution median is 2.3

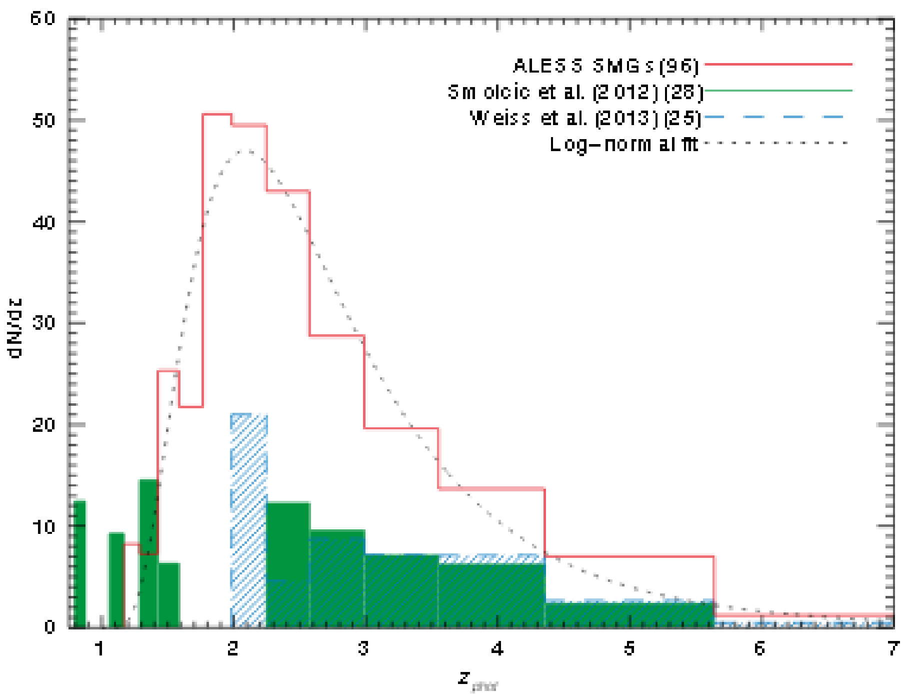

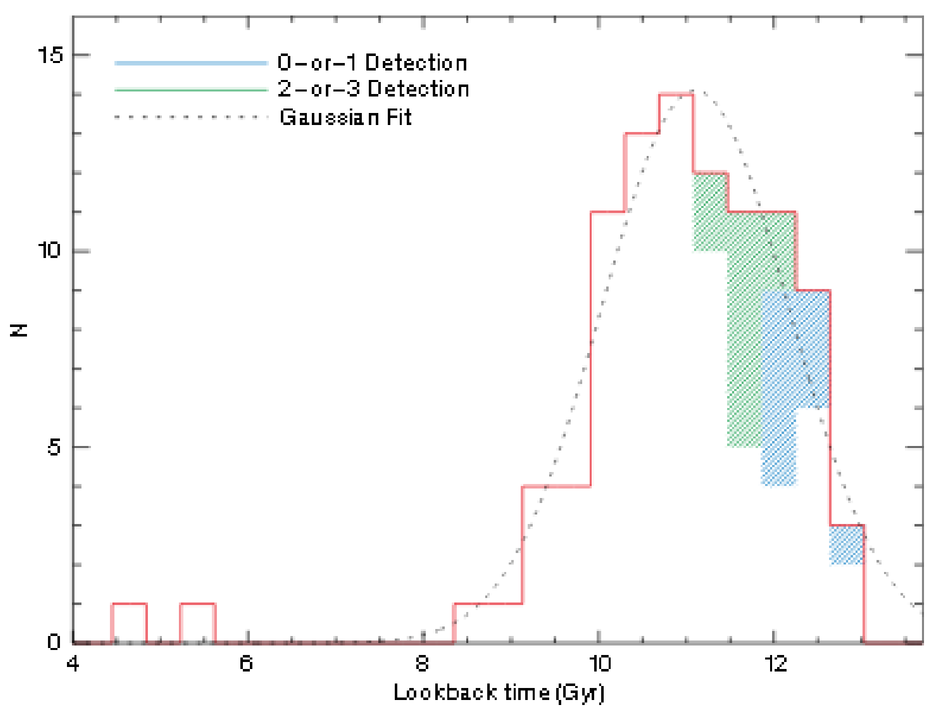

Simpson et al. 2014, Smail et al 2015

Lensed galaxies

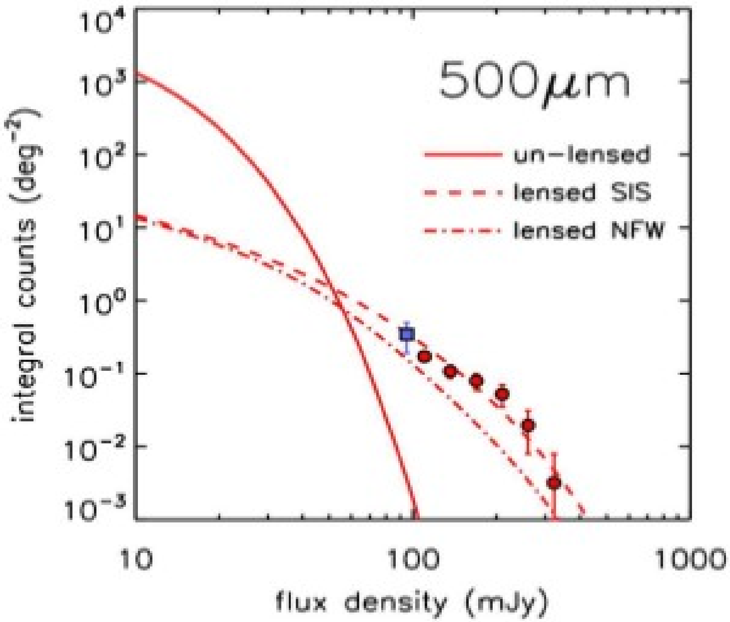

Gravitational lensing: magnifies (in flux and size) the observability of “normal” galaxies
Observing high-z lensed :
-to constrain model of galaxy formation
-to measure galx evolution up to high-z
-to investigate high-z gal physical properties

All z=1 dust-obscured star forming gal in submm above 100mJy at 500micron are boosted by lensing (by a factor 10) (Negrello et al. 2010) in H-ATLAS SDP 5 lensed in 135sqdeg (all survey 400sqdeg)
Lensed images separated by 1-2 arcsec

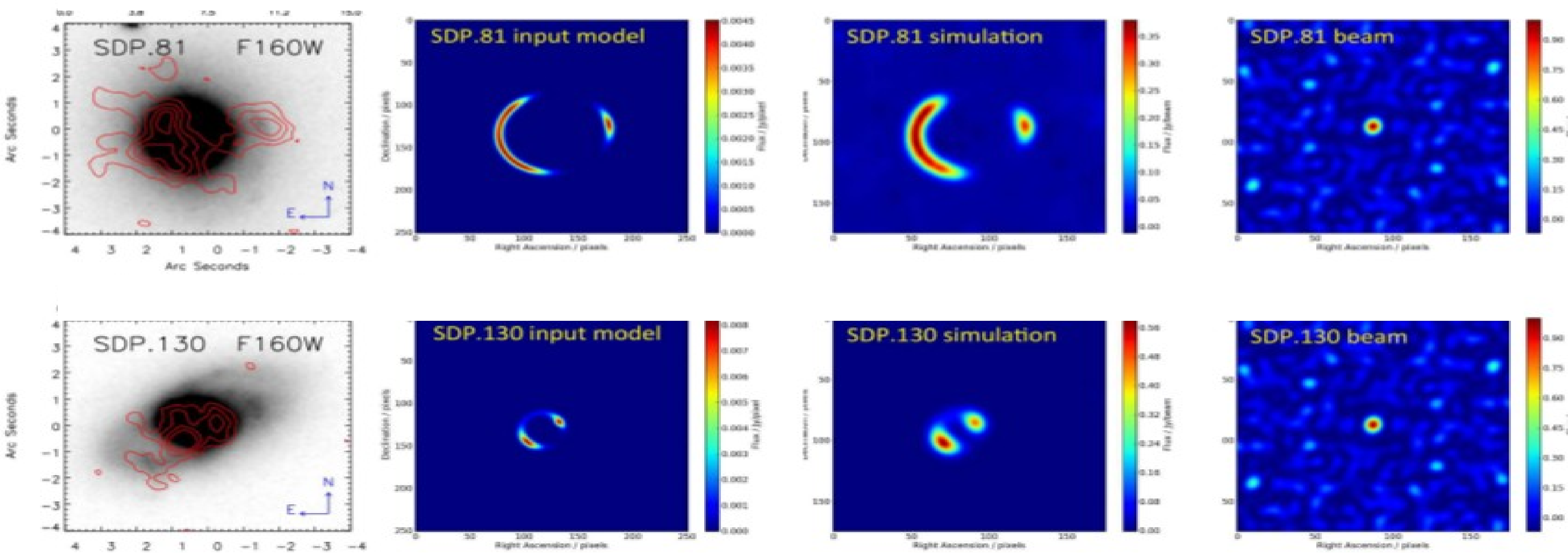

SMA 345 GHz model of lensed ALMA Cycle 0: 20 min in ext config

ALMA Observations of SPT Discovered, Strongly Lensed, Dusty, star-forming Galaxies

Hezaveh et al 2013; Vieira et al 2013; Weiss et al. 2013

PI: D. Marrone

NIR Images + ALMA (Band 7) 870 μm Contours

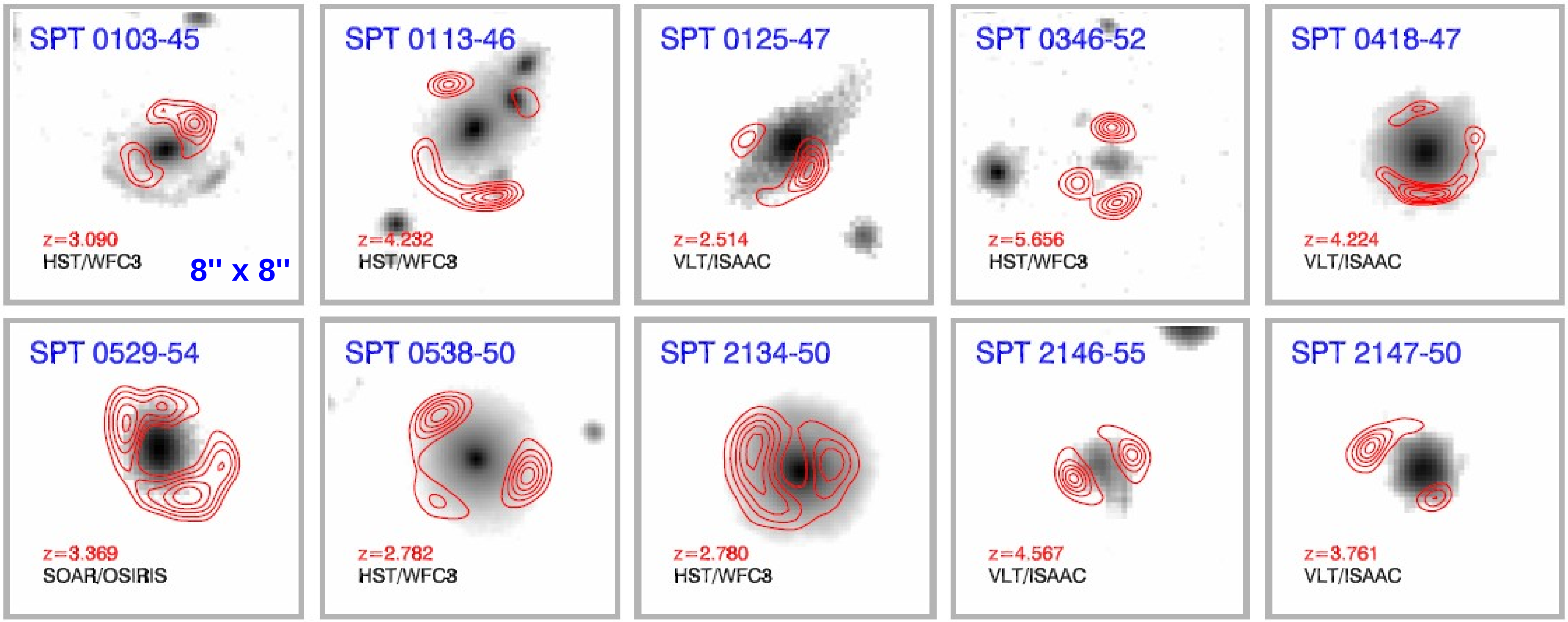

OBSERVATIONS

- ~15 antennas,
- ~4 hrs (~80 sec/source)
- Band 3 (spectroscopy)
- Band 7 (imaging)
- Resolution ~ 1.5''

Catalog of z > 1 strongly gravitationally lensed sources sampled from the South Pole Telescope (SPT) survey

47 SMGs detected with SPT, F(1.4 mm) > 20 mJy

Multiple images, separated by 1-3": **consistent with strong lensing**

Magnification Factors: 4-22

Lensed sources = ultra luminous starburst galaxies at high z

ALMA allows to image lensed galaxies obscured in NIR/optic where the lens dominates the emission

ALMA Observations of SPT Discovered, Strongly Lensed, Dusty, star-forming Galaxies

Hezaveh et al 2013; Vieira et al 2013; Weiss et al. 2013

PI: D. Marrone

First spectroscopic redshift survey with ALMA

ALMA Cycle 0 Band 3
100 GHz compact configuration
26 sources
5 tunings in the 3 mm band
10 minutes per source

- Spectral lines in 23 out of 26 sources
- Multiple lines in 12 of 23 sources
- At least 10 sources at z > 4

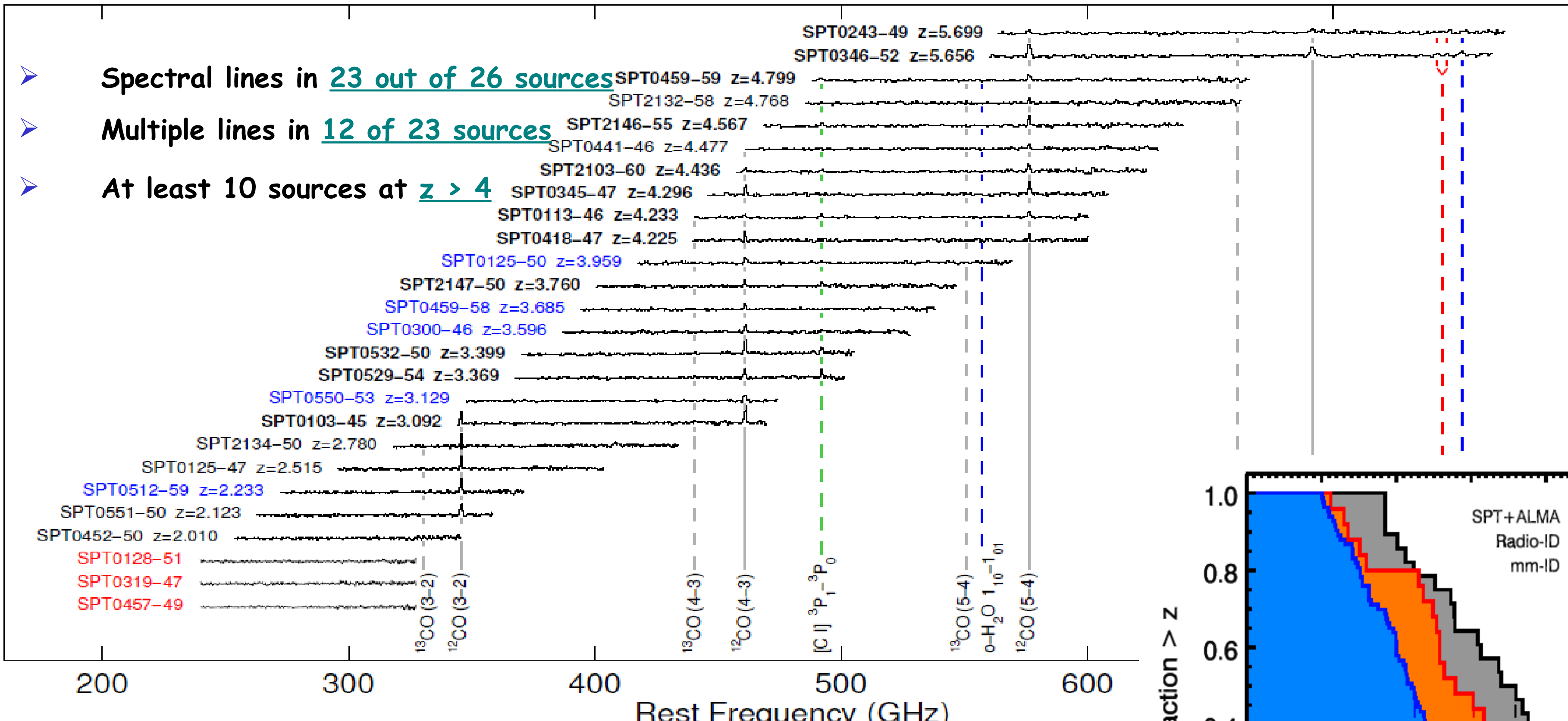

Bold = unambiguous redshift from ALMA
black = single lines with ALMA, confirmed with C+ or CO(1-0) with APEX or ATCA
blue = single line detected with redshift, most likely redshift from photo-z
red = no line detected

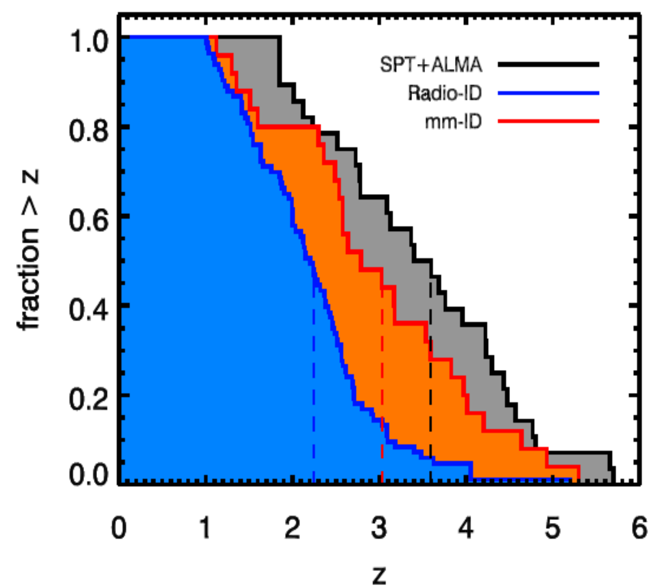

ALMA Observations of SPT Discovered, Strongly Lensed, Dusty, star-forming Galaxies

Composite rest frame spectra of 22 high-z SMG

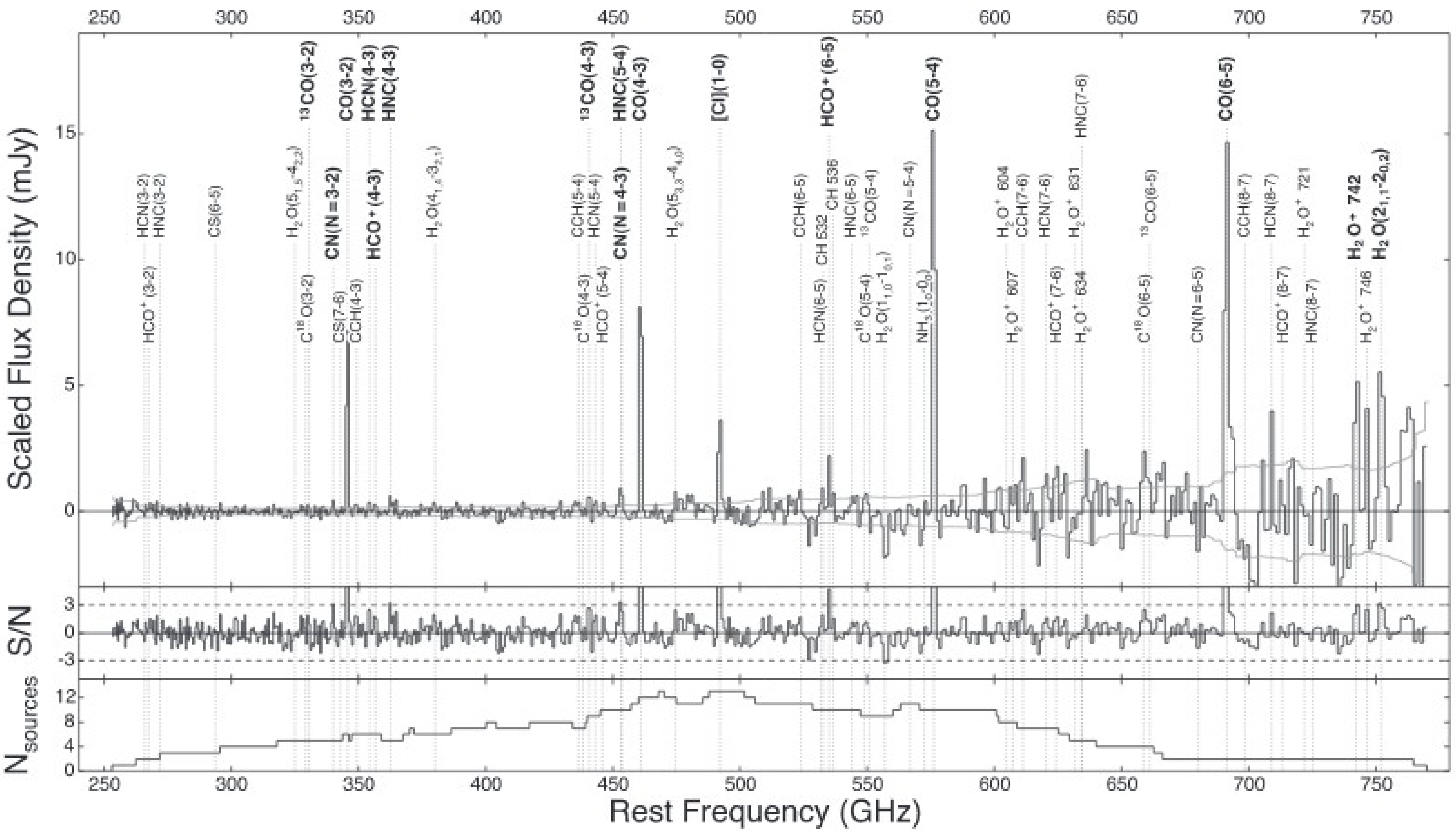

Spilker et al. 2014

Sdp.81

HATLAS J090311.6-003906 in a gravitationally lensed submm galaxy at z=3.042 lensed by an elliptical galaxy at z=0.299

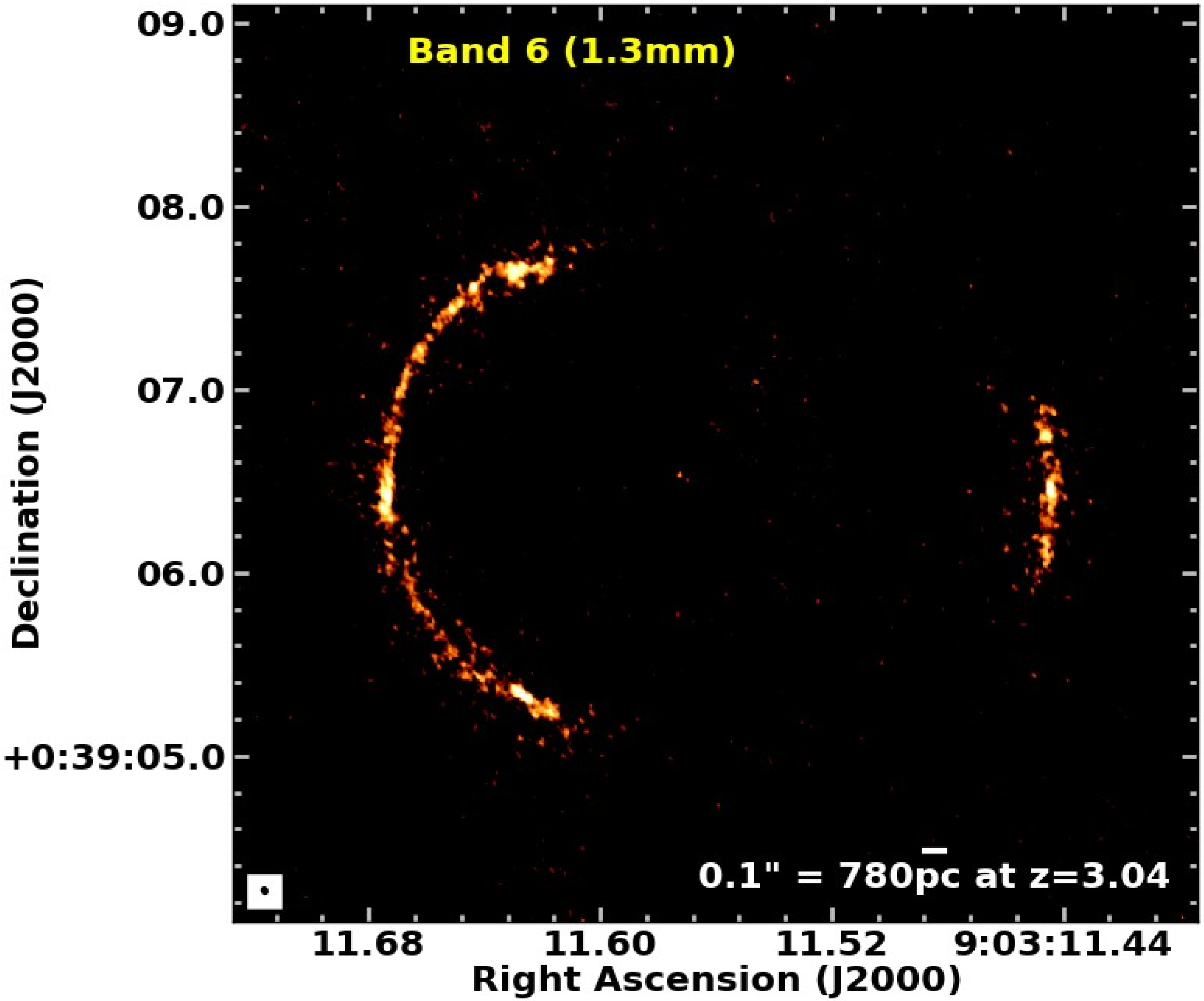

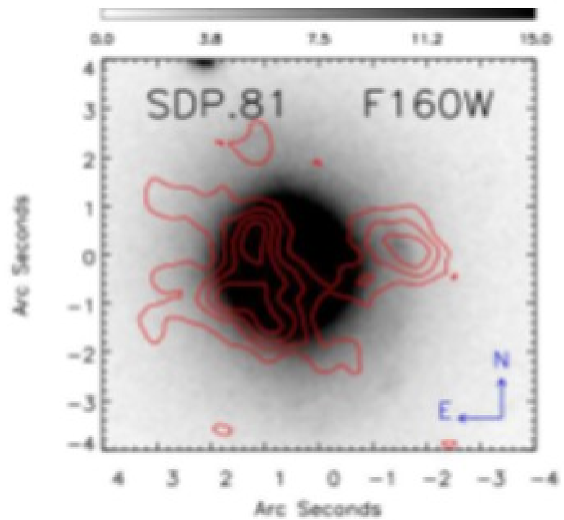

- Science Verification
- ~22-35 antennas,
- ~9-12hrs/band
- Band 4,6,7 (CO5-4. H2O, CO8-7, CO10-9)

(ALMA partnership 2015)

Resolution 60 x 54 mas, 39 x 30 mas and 31 x 23 mas in Bands 4, 6, and 7 (20-80x better than SMA and PdBI) corresponding to few tenth of pc in source plane

Sdp.81

Continuum emission

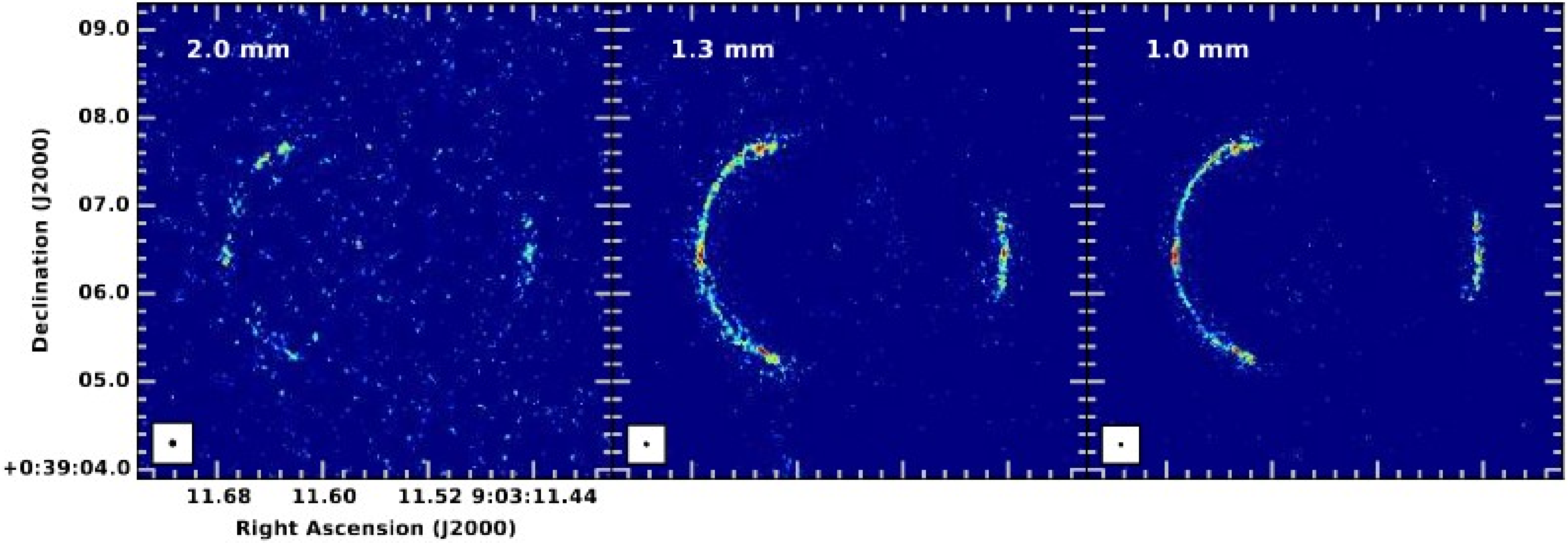

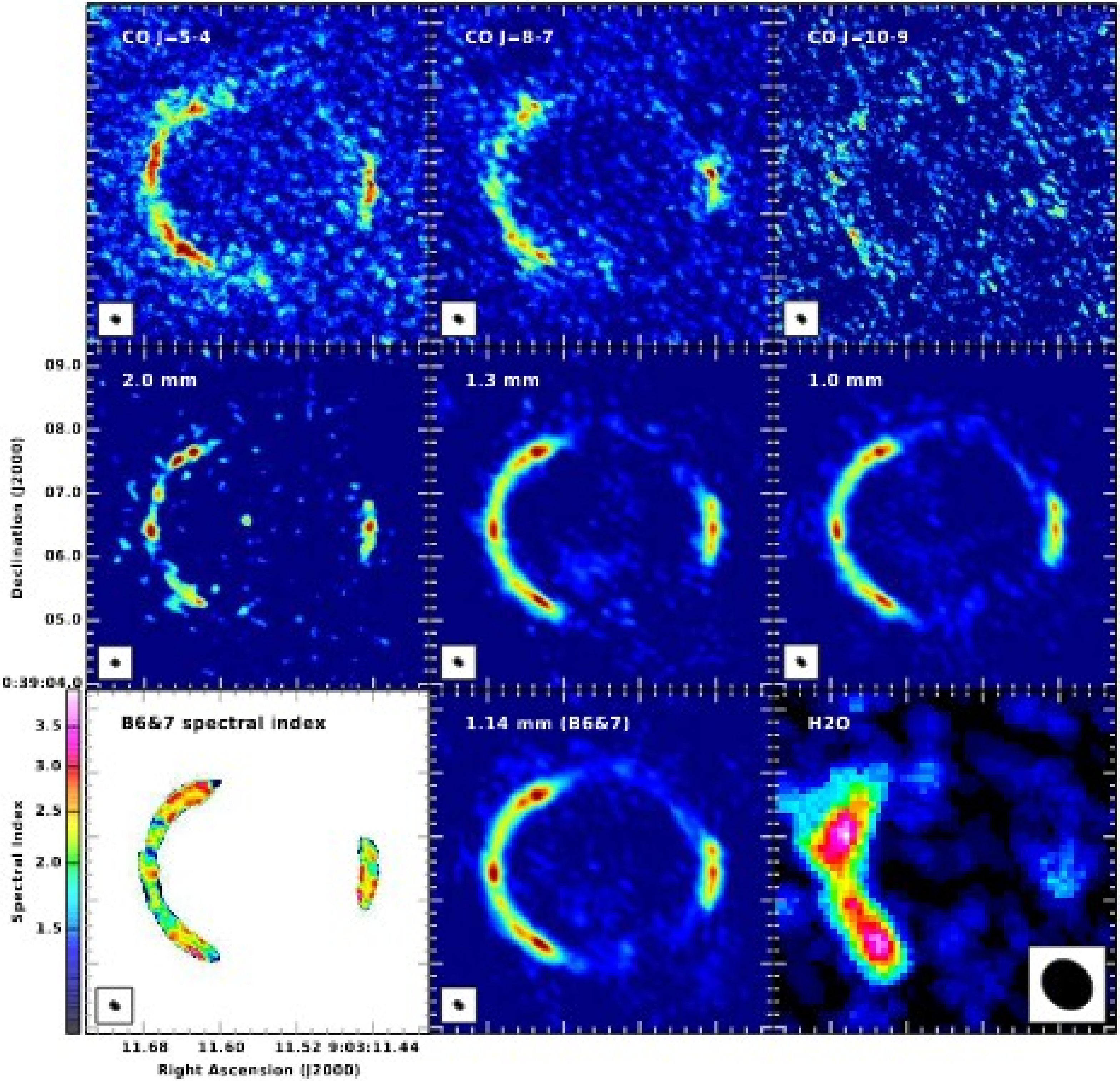

CO J=5-4
CO J=8-7
CO J=10-9
2.0 mm
1.3 mm
1.0 mm
B6&7 spectral index
1.14 mm (B6&7)
H2O
Declination (J2000)
09.0
08.0
07.0
06.0
05.0
+0:39:04.0
Spectral Index
3.5
3.0
2.5
2.0
1.5
11.68
11.60
11.52 9:03:11.44
Right Ascension (J2000)

Sdp.81

B6 & B7 model reconstruction

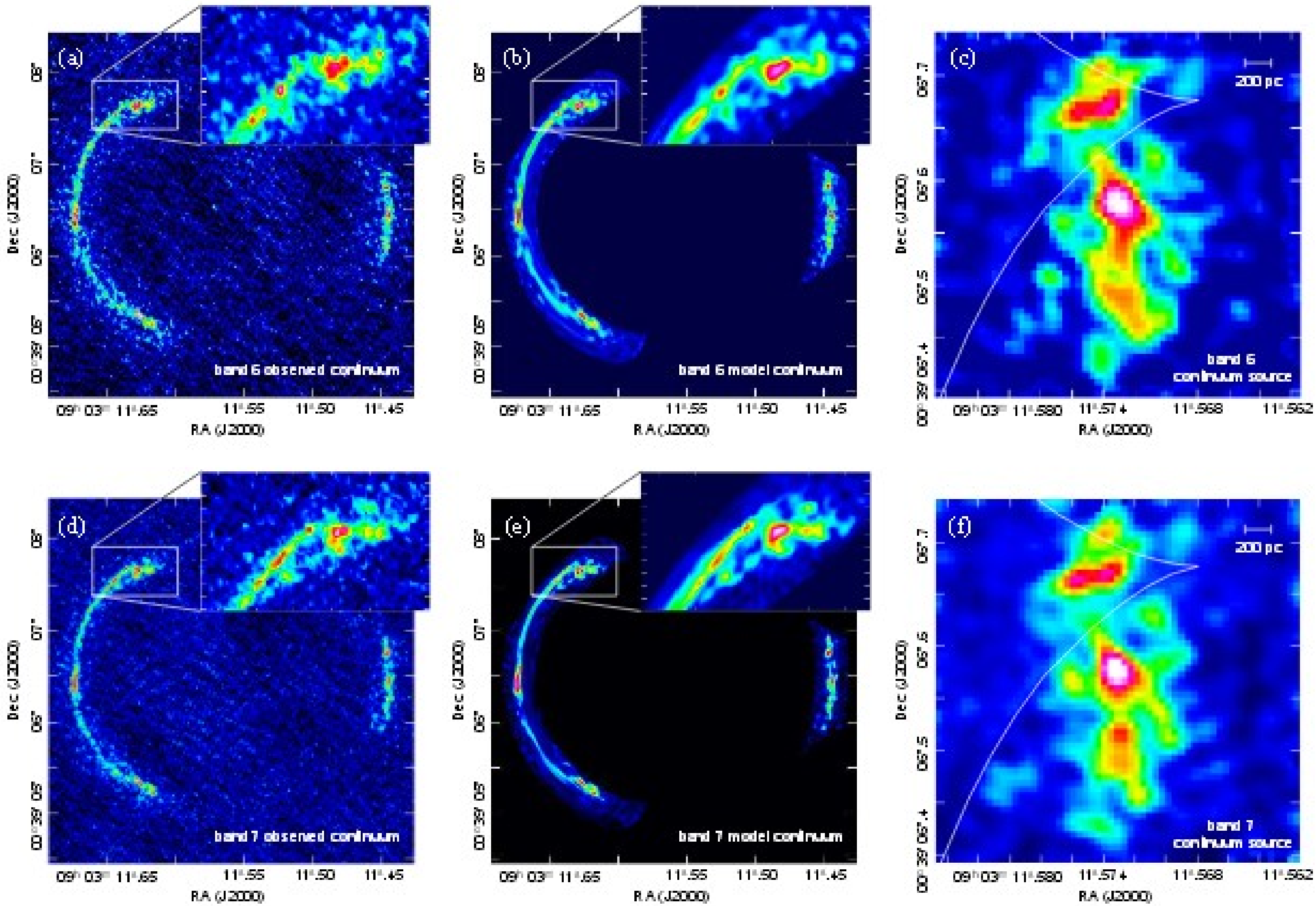

(Dye et al. 2015)

Outline

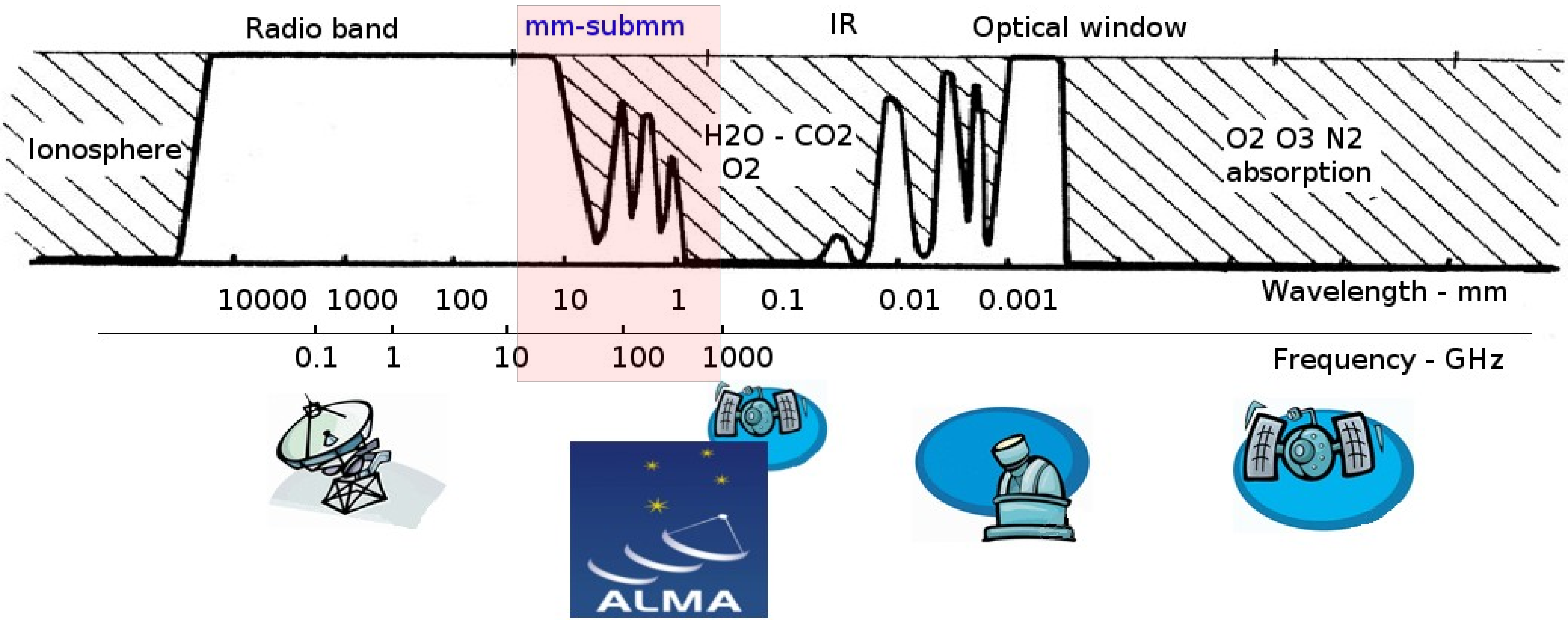

Observing instruments: **Interferometers (ALMA)**

Science topics

Science cases

Observing processes: **Proposals and archives**